Desalination and Water Treatment
www.deswater.com
doi: 10.5004/dwt.2022.28031

246 (2022) 174–195
January

Fabrication and characterization of porous ceramic composite membrane for water and wastewater treatment

A.A. Oyekanmi[a], Abdul Khalil H.P.S.[a,*], T.T. Dele-Afolabi[b], Mohd Rafatullah[a], Mohammed R.M.S.[c,*], Tata Alfatah[a], Danish Mohammed[a], C.K. Abdullah[a]

[a]*School of Industrial Technology, Universiti Sains Malaysia, Penang 11800, Malaysia, emails: akhalilhps@gmail.com (Abdul Khalil H.P.S.), abdulkan2000@yahoo.com (A.A. Oyekanmi), mrafatullah@usm.my (M. Rafatullah), tataalfatah83@gmail.com (T. Alfatah), danish@usm.my (D. Mohammed), ck_abdullah@usm.my (C.K. Abdullah)*
[b]*Department of Mechanical and Manufacturing Engineering, Universiti Putra Malaysia, 43400, UPM Serdang, Selangor, Malaysia, email: deleafolabitemitope@gmail.com (T.T. Dele-Afolabi)*
[c]*Faculty of Civil Engineering and Built Environment, Universiti Tun Hussein Onn Malaysia 86400, Malaysia, email: maya@uthm.edu.my (Mohammed R.M.S.)*

Received 2 June 2021; Accepted 27 November 2021

ABSTRACT

Ceramic based composite has attracted remarkable interest due to its pore structure that enables pollutants removal from water and wastewater treatment including inherent thermal and chemical stability. Detailed studies towards the improvement of pore networks of ceramic composites in terms of cost effective fabrication and characterization techniques for water and wastewater treatment is the focus of this study. This review introduces different forms of ceramic composites including alumina, mineral based ceramic composites, silica derived ceramic composites, titanium ceramic composites, zirconia, zeolite and oyster shell based composites for improved application for water and wastewater treatment. Fabrication methods which includes pore-forming agent technique, vacuum impregnation process and 3D gel printing have shown ample viability for the development of highly robust porous ceramic composite membranes with tailored porosity. The removal of organic and inorganic pollutants from water and wastewater was attributed to improved pore structure of ceramic composites. The high stability, durability and low fouling including high flux exhibited by ceramic composites indicated its prospects for water and wastewater treatment. The article reviews the synthesis of ceramic based composites and their functional properties with the aim of providing literature support for future applications.

Keywords: Fabrication; Characterization; Ceramic composites; Water treatment; Wastewater treatment

1. Introduction

High production of effluents especially from industries have increased research methods for wastewater treatment in order to minimize the effect of water and land pollution as a result of discharge to the environment and the receiving water [1]. Industries such as agro-allied, mining and smelting, pulp and paper, pesticides, soap and detergents generate very high amount of wastewater. As a result, effective treatment methods to remove pollutants from wastewater remains a challenge to environmental scientists and engineers in most of the developing countries in the world [2]. Some of the conventional wastewater treatment technologies include coagulation, ion-exchange, reverse osmosis, nanofiltration and adsorption [3]. Among these treatment methods, adsorption is considered cost

---

* Corresponding authors.

effective and environmentally friendly due to its large surface area and the porous nature of the adsorbents for the permeation of pollutants. Even though, membrane fouling is a dominant factor that restrains the membrane performance in prolonged operation, the choice of membrane materials, the tailoring of the membrane pore size and the pore size distribution can effectively mitigate the fouling induced by the obstruction of pores [4–6]. Recently, with the advancement of broad based strategic industrial processes for wastewater treatment, there is urgent need for substitute high-performing porous membranes adsorbents of high mechanical stability, ion exchange characteristics, high removal capacity and regeneration potentials that can sufficiently meet the demands of these technologies, which also can be a suitable alternative to conventional treatment methods [7–11].

For this purpose, ceramic membranes have been found to be the preferred candidates relative to polymeric membranes due to: (i) a relatively narrow pore size distribution and higher porosity, leading to excellent separation capacity and a higher flux, (ii) superior mechanical stability (giving room for greater pressures), (iii) superior chemical stability leading to longer lifespan of the membrane, and (iv) superior hydrophilicity leading to high fluxes at lower pressures and lower fouling [12].

The application of low cost ceramic-based adsorbents have been widely reported in the literature. For example, Vo et al. [13] reported the adsorption of ammonia on a mesoporous alumina membrane. The authors revealed that the sorption capacity was enhanced by the textural properties of the adsorbent [14,15]. Similarly, Kim et al. [16] have investigated the uptake capacity of bed shaped alumina membrane with tunable particle size for the removal of ammonia, the authors revealed that optimum adsorption efficiency was achieved using the least particle size. Khan et al. [17] have reported that chemical modification of alumina using HCl and NaOH increased the sorption capacity of the adsorbent for the removal of emerging pollutants such as acrylic acid. The authors attributed the removal efficiency to non-spontaneous exothermic adsorption process that occurred within the solid-solution boundary. Suganuma et al. [18] investigated the adsorption efficiency of amorphous silica-alumina for the removal of nitrogen from heavy oil. It was revealed that pore diffusion of compounds can be attributed to the sorption capacity [19].

Even though the excellent synergy and interaction between the ceramic matrix structures and the pore networks have made the traditional porous ceramic materials as an ideal choice, the intrinsic brittleness including great sensitivity to post-fabrication machining have restrained the prospects of porous ceramic membrane as ideal materials for numerous load-bearing applications and extreme operational conditions [20–22]. By way of illustration, alumina ceramic (Al_2O_3) has significant chemical and high mechanical strength and stability but have low thermal shock resistance [23,24]. Therefore, in spite of being a leading porous ceramic material, plain alumina ceramics are yet to sufficiently exhibit the necessary functional properties to withstand the passage of time and also working under the detrimental effect linked with shocks from sudden thermomechanical loading. As a consequence, it becomes essential for academics and industrial operators to rework the conventional porous ceramics so as to enhance their mechanical and functional features properties for water wastewater treatment. He et al. [25] studied the use of ceramic membrane for the treatment of water and wastewater. The drawback in their study lies in the high fabrication cost of precursors and lack of in-depth fabrication techniques capable of enhancing the performance and long service life of the membranes.

To address these problems, recent investigations have revealed that the composite approach as an effective way to rework the traditional porous ceramics by developing porous ceramic composites through the powder consolidation and chemical based techniques such as the utilization of particulate (e.g., metals, polymers and multi-phasic ceramics) and fiber (e.g., carbon nanotubes and graphene nanosheets) reinforcements. In recent years, the hierarchical porosity of ceramic based composites have become subject of intensive review [26]. However, no review study have been reported on the intrinsic functional properties and fabrication techniques of enhancing the performance of porous ceramic composite for wastewater treatment. Therefore, in order to gain deeper insight into the research progress made thus far with the implementation of the composite approach to rework traditional porous ceramics, this study gives detailed information on the different processing techniques for the synthesis of porous ceramic composites and the various characterization techniques for the evaluation of the properties of porous ceramic composites. This review comprehensively discuss the application of ceramic composite including the strengths and limitations under different categories of ceramic composites for the removal of pollutants from water and wastewater. This study on porous ceramic composite is focused on activated alumina, modified alumina and mineral based alumina composites. There are works in the literature which are solely confined to the application of composite membranes for the stated purpose of pollutant removal from water and wastewater. However, the synthesis and application of ceramic composites membranes has evolved in the frontline for wastewater treatment. The authors wish to recommend that the potential and capacity of the ceramic composite materials is based on the operational parameters of the experimental set and the impact on the type of wastewater investigated.

2. Overview of processing techniques

Porous ceramic membranes have found immense application in several industrial technologies including thermal insulation, fuel cell technology, catalyst support, wastewater treatment and others [27–31].

In recent years, the application of ceramic membranes for water purification via membrane distillation has been extensively discussed. The efficiency of the treatment process can be attributed to their excellent chemical, thermal and structural stabilities. Most ceramic membranes are made from metal oxides such as alumina and silica which are hydrophilic in nature because of the presence of hydroxyl (OH^-) groups on the surface. This surface behaviour inhibits them from being used up in the process of membrane distillation. In some instances surface modification is required to improve on the hydrophobic surface ceramic composite. Fang et al. [32] prepared a hydrophobic porous alumina from hydrophilic hollow fiber through grafting with fluoroalkylsilane for water desalination. The performance efficiency of the hydrophobic fiber was determined by vacuum membrane distillation.

Dele-Afolabi et al. [33] prepared porous ceramic composites using alumina as the ceramic matrix and nickel as the metal reinforcement including agricultural waste materials such as rice husk (RH) and sugarcane bagasse (SCB) as pore-forming agents (PFA). Relative to the problem of homogenization experienced in some other ceramic reinforcements, nickel particles were uniformly distributed in alumina via wet milling in ethyl alcohol and subsequently dry milled to crush lumps from dried slurry. Meanwhile, before the pore-forming materials were included. Locally sourced agro-waste pore formers (RH and SCB) were pulverized, leached in 1M HCl solution and were sieved to achieve a particle size in the range of 63–25 μm. After preparing the PFA, both the composite blend and pore former powders were obtained by dry milling and thereafter they were exposed to a manual mixing using an agate mortar to homogenize the sucrose solution binding agent and the powder blends. Afterwards, the samples were compacted at 95 MPa and exposed to an optimal heat treatment on the basis of the thermal properties of the PFA. The organic burnout process was first performed on the green pellets for the PFA decomposition and thereafter sintered at 1,450°C. The sintering temperature profile was to ensure a bearable viscosity level of the Ni melt (melting temperature of nickel = 1,450°C) and also to reduce the extrusion of the reinforcement of Ni during sintering. A schematic for the fabrication of the Ni-reinforced porous alumina composites is illustrated in Fig. 1.

Wang et al. [34] employed a special two-step sintering technique to develop porous ceramics of aluminum titanate-strontium feldspar-mullite (ASM) ternary composite. The procedure involved the preparation of Al_2TiO_5 clinker by mixing Al_2O_3 and TiO_2 powders in ethyl alcohol medium and subsequently calcined at 1,550°C for 3 h. To prepare the strontium feldspar ($SrO \cdot Al_2O_3 \cdot 2SiO_2$), Al_2O_3, $SrCO_3$ and TiO_2 powders were mixed in ethyl alcohol medium and subsequently calcined at 1,400°C for 3 h. Thereafter, the ASM ternary composite having 70% Al_2TiO_5 clinker, 25% $SrO \cdot Al_2O_3 \cdot 2SiO_2$ and 5% mullite fiber ($3Al_2O_3 \cdot 2SiO_2$) was mixed with potato starch pore-forming agent for 4 h. The powder blend was dry-pressed, dried and was later sintered by the two-step sintering technique to obtain the ASM porous ceramic composites.

Khattab et al. [35] prepared porous alumina-felsite ceramic composites using coagulation casting method consisting of samples of alumina using different weight ratio of felsite powder (0, 10, 20, 30 wt.%) alongside 0.6 wt% ACT based on powder and 0.6 mol/L of urea (catalyst) were

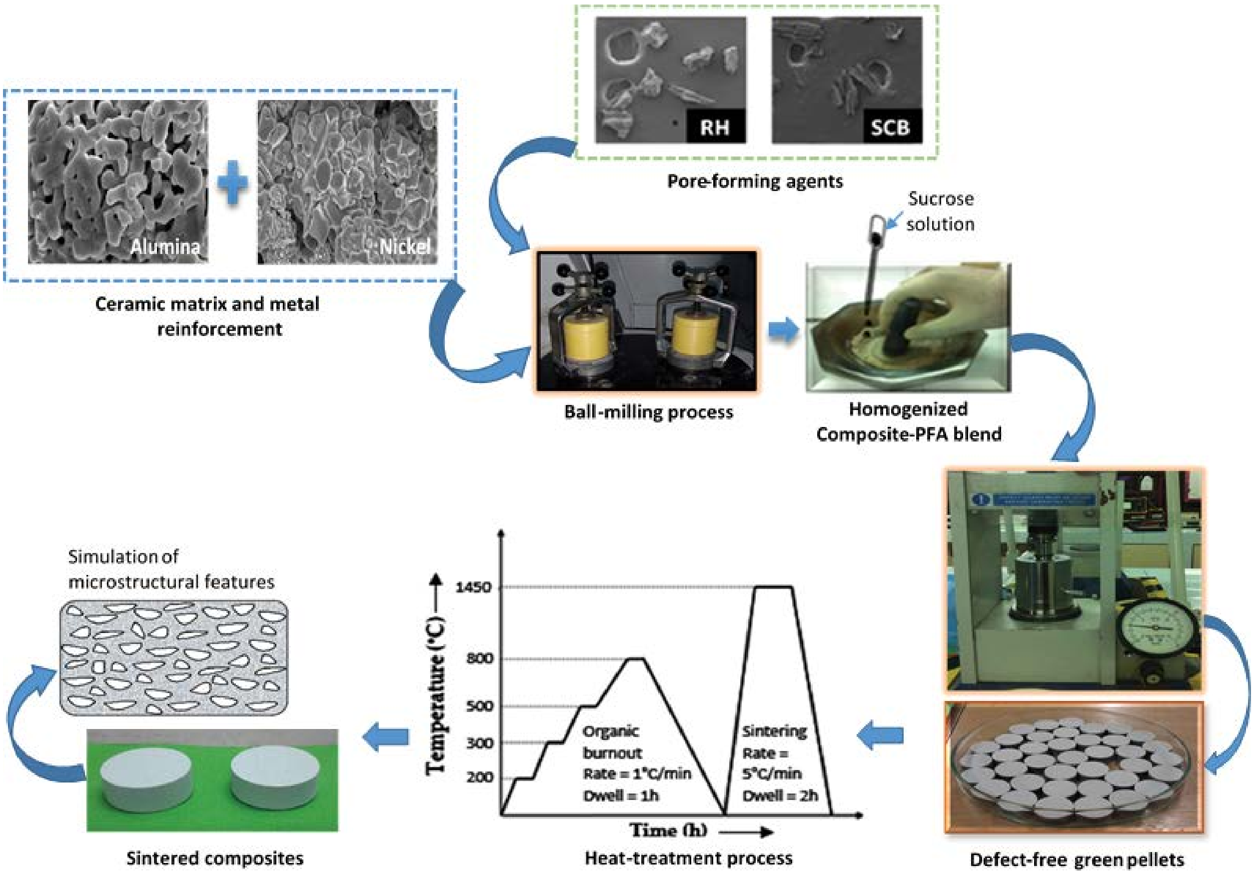

Fig. 1. Schematic for the fabrication of the Ni-reinforced porous alumina composites [33].

employed in preparing the suspended ceramic slurries. Acidic slurries were prepared at pH 4 by introducing H_2SO_4 acid. Urease was employed as an enzyme for shifting the pH of acidic slurries from 4 to 9. Activated urease enzyme reacted with urea and raised pH which induced coagulation. Afterwards, samples were remolded, dried for 7 d at 25°C and 90% relative humidity and sintered at 1,550°C, 1,600°C, and 1,650°C.

Highly permeable ceramic thin film composite hollow fiber membranes (HFMs) prepared through graphene oxide (GO) pre-coating technique was reported by Cho et al. [36]. The entire coating processes for developing the ceramic composite HFMs with sacrificial GO layer (AG-HFM) are presented in Fig. 2. In order to develop the GO interlayer-coated HFM (G-HFM), the dispersed GO was diluted with ethyl alcohol at ratio 1:1 to produce a uniform GO layer on the support HFM. The prepared GO solution was coated on the HFMs support using a simple dip-coating method. The G-HFM was dried for 1 h at ambient temperature prior to coating with boehmite sol. In addition, γ-alumina active layer was prepared by similar dip-coating process. Lastly, the dried samples were calcined at various temperatures for the preparation of active layers with various pore sizes. The samples were vertically placed in a muffle furnace and fired up to the final temperature (200°C–1,000°C) at heating rate of 1°C/min and were then cooled naturally.

Li et al. [37] prepared Si_3N_4-SiCN ceramic composite foams consisting of hierarchical pore structure using protein-based gelcasting and infiltration of precursor and pyrolysis (PIP). Preparation of the porous ceramic composites began with gelcasting process where the raw materials having weight ratio of 94:3:1.8:1.2 (Si_3N_4:SiO:Y_2O_3:Al_2O_3) were adequately milled with 10 wt% which was relative to the powder mixture, egg white powder, followed by the addition of distilled water stepwise. Subsequently, the mixtures were ball milled to produce ceramic slurry. Thereafter, pouring of the slurry into the mold was achieved and was maintained at 80°C in a water bath to produce the ceramic gel. The gel was completely dried and then placed in the oven. Lastly, dried gel was burnt out at 600°C for 1 h to eliminate the organic materials and finally the porous Si_3N_4 green samples were produced. The PIP process was performed through the infiltration of the porous Si_3N_4 green samples by PSZ-50 solution (n-hexane solvent) after which the solvent of the solution was eliminated by heating in the oven and by curing simultaneously at 220°C and 250°C. The pyrolysis and pressureless sintering were then performed by heating samples to 800°C within 3 h of pyrolysis and then to 1,500°C–1,650°C for 2 h of sintering.

For the purpose of characterizing the mechanical properties and also in vitro response of a porous ceramic composite bone tissue scaffold, Guzzo and Nychka [38] developed the composite scaffolds by utilizing bioactive glass frit and aqueous sodium silicate liquid. Unannealed melt-cast 45S5 bioactive glass frit was employed as matrix for developing the composite scaffolds. Two different scaffolds were developed, discs (10 mm diameter; 2.7 mm height) and right cylinders (12 mm diameter; 27 mm height). The smaller disc specimens were utilized for in vitro investigation and the mechanical performance was investigated using larger right cylinders. Pastes having similar quantity of frit and different fractions of binder phase (18, 25, and 32 wt.%) were produced so as to determine the binder amount influence on structure along with mechanical and in vitro behavior. Porous hydroxyapatite ceramic (PHC)-based composite phase change materials (PCMs) were prepared by Wu et al. [39] using the vacuum impregnation process. Firstly, the PHCs and solid PEG were fixed in a closed glass vessel. The vessel was thereafter removed using a vacuum pump. During this period, the vessel was placed in the water bath and was heated up to 70°C to melt the PEG in order to allow it to completely infiltrate the PHC. Lastly, the composite was removed and allowed to cool on a filter paper. For the purpose of removing the remaining PEG on the PHC surface, it was placed in an oven (70°C) and the filter paper was replaced multiple times until no PEG was left on the filter paper.

Shao et al. [40] successfully developed porous $CaSiO_3$-$CaSO_4$ composite scaffolds using 3D gel-printing (3DGP) technology. As seen in Fig. 3, the slurry of the composite powder prepared. Thereafter, the computer sliced the 3D model via the slicing software followed by layer-by-layer printing of the green body. Lastly, the green body was fired to obtain the composite scaffold. Porous chitosan/ZnO-doped bioglass composites were developed using chitosan solution and ZnO-doped bioglass from CaO-SiO_2-P_2O_5

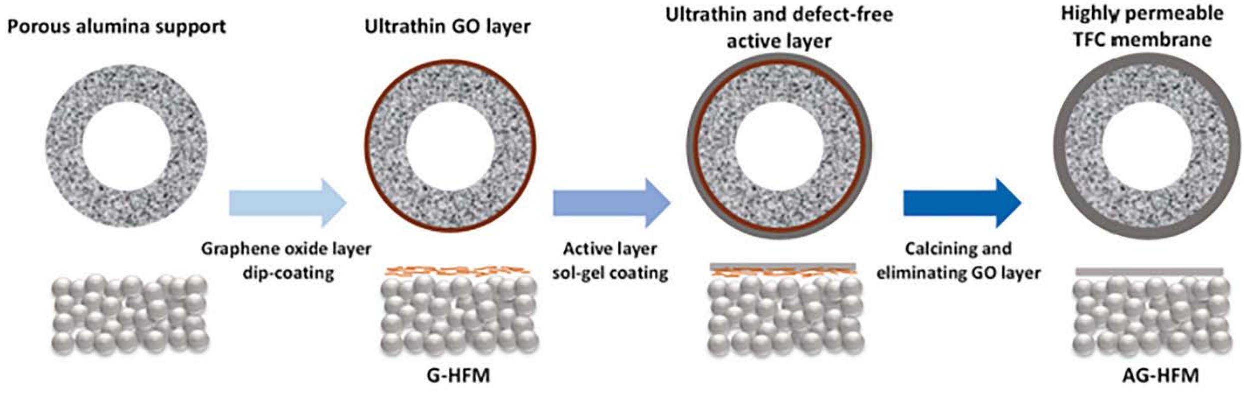

Fig. 2. Schematic representing developing the ceramic composite HFMs with sacrificial GO layer (AG-HFM) [36].

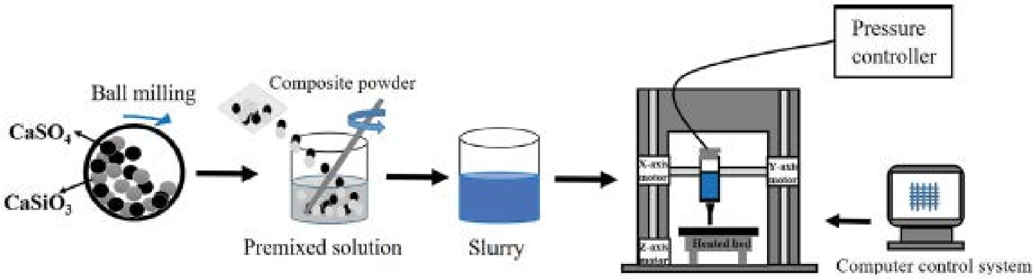

Fig. 3. Schematic representation of 3DGP process for porous composite scaffolds [42].

system [41]. The composites were obtained through lyophilization of stable dispersions formed by mixing of 2% chitosan solution in acetic acid solution with bioglass grains so as to maintain 1:1, 1:3, and 1:5 bioglass and polymer weight ratio. The lyophilization process was performed by freezing and sublimation of the solvent using the Christ BETA 1-16 lyophilizer.

In summary, the investigations discussed above highlight relatively cost-effective fabrication techniques for developing ceramic composite membranes. Indeed, powder metallurgy technique seemed more economically viable for the development of porous ceramic composites using pore-forming agents from natural organic matters since the high immiscibility factor of these materials with ceramic slurry makes the application of other techniques more challenging. Meanwhile, coagulation casting method has proven to be highly promising for mass production of porous ceramic composites with complex shapes, high strength and high reliability. Defects can be eliminated to a large extent due to easy control of particle-particle interactions and increased packing density in the wet stage relative to dry processing. However, due to the existence of various chemical pathways, different strengths are exhibited by the bonds between the coagulated ceramic particles. Three-dimensional (3D) gel-printing technology has made the fabrication of ceramic composite membranes with arbitrarily complex shapes possible. However, this technique is more expensive relative to other techniques discussed above and industrial mass production of ceramic composite membranes with larger size is quite challenging owing to the intrinsic brittle nature and low expansion coefficient of ceramic-based materials. With the vacuum impregnation process, uniform distribution of pore sizes can be achieved, nonetheless, the difficulty in controlling the pH value and temperature of precipitation can adversely affect the developed ceramic composite membranes using this system.

3. Characterization of porous ceramic composites

3.1. Porosity and microstructural characterization of porous ceramic composites

The adequate control of parameters of porosity is very critical in maintaining remarkable strength integrity in porous ceramic composites. So far, numerous researchers have utilized the method of linear intercept using ASTM E112 [43] and mercury porosimetry [44] for measuring the pore structures, while the parameters of density and porosity of the porous ceramic composites have been measured using the Archimedes' principle (ASTM C20) as presented in the equations below [45]:

$$\rho = \frac{m_{\text{dry}} \times \rho_{\text{water}}}{m_{\text{wet}} - m_{\text{suspended}} + m_{\text{wire}}} \tag{1}$$

$$P_{\text{open}} = \frac{m_{\text{wet}} - m_{\text{dry}}}{m_{\text{wet}} - m_{\text{suspended}} + m_{\text{wire}}} \times 100 \tag{2}$$

$$P_{\text{total}} = \left(1 - \frac{\rho}{\rho_{\text{theoretical}}}\right) \times 100 \tag{3}$$

where m_{dry} denotes dry mass of sample, $m_{\text{suspended}}$ indicates mass of the sample suspended in water, m_{wet} represent mass of sample after soaking m_{wire} signifies mass of the suspending system, ρ_{water} represents density of water, P_{total} illustrates volume fraction of total porosity of sample and P_{open} is the fraction of volume of open porosity of the sample, $\rho_{\text{theoretical}}$ indicates theoretical density.

Researchers have utilized metallographic method for sample preparation for many years in preparing porous ceramic composites for detailed microstructural evaluation. Porous ceramic composites using this technique are subjected to different processes in the order of grinding, polishing, etching and microscopic evaluation. Considering the preponderance of surface deformities as well as the fragile nature of pore cavities in the sintered porous ceramic composites, it is important to utilize the fine grinding (1,200 and 4,000 mm SiC papers) and polishing processes to prepare samples free from scratches, cracks and most importantly to avoid having blocked pores. In spite of being optional, etching is carried out to achieve plain microstructure with respect to the polished sample by utilizing the chemical etching technique (very strong and hazardous reagents) or the thermal etching technique (heating up polished sample up to approx. 200°C of the sintering temperature) [46]. The most popular microscopic technique which can be utilized for microstructural examination of porous ceramic composites is the electron microscope including the scanning electron microscope (SEM) and the transmission electron microscope (TEM). The SEM is frequently used for viewing and measuring the microstructure and the pore structures of porous ceramic composites respectively. More so, sputter coating of the specimen with ultra-thin electrically conductive metals such as gold, platinum, silver, chromium etc., is needed owing to their low electrical conductivity of ceramic matrix and the presence of pore structures that quickens the build-up of electrostatic charges hence, resulting to electron beam deflection and charging effect. The coating functions as the conductive metal layer on the porous ceramic composite sample is to obstruct charging effect and to enhance secondary electron signal which is needed for the microstructural examination in the scanning electron microscope. Meanwhile, the granular microstructure of porous ceramic composites, particularly, the ones reinforced with metals can be examined by utilizing the transmission electron microscope. In order to conduct this analysis. The focused ion beam (FIB) with the SEM of a dual beam system are utilized in producing a high quality electron transparent membrane (lamella thickness of approx. 80 nm) from the coated porous ceramic composite specimen (Fig. 4). After selecting a spot of interest, the ion beam is then utilized to deposit approximately 0.5–1 mm thick metal line (Fig. 4a). Thereafter, high beam current is employed to mill bulk materials from the spot of interest, leaving out only a tab of material to hold the specimen (Fig. 4b). By using a micromanipulator tip, the thin lamella sample is eliminated and positioned on a copper grid as shown in Fig. 4c and d, respectively. A magnified micrograph of the porous ceramic composite specimen for TEM analysis is shown in Fig. 4e. Fig. 5a and b show the SEM and TEM microstructures of rice husk-shaped Ni-reinforced porous alumina composite respectively.

3.2. Mechanical properties characterization of porous ceramic composites

Several researchers have employed three different types of mechanical properties test for the characterization of porous ceramic materials which includes Brazilian disk test, compression test, hardness test and flexural strength test.

3.2.1. Brazilian disk test for porous ceramic composites

The Brazilian disk test (also called diametral compression test or indirect tensile test) is one of the major tests utilized in measuring the tensile strength (Fig. 6) of brittle materials such as rocks, concrete, polymers and ceramics [48,49]. ASTM D3967 and ASTM C496/496M explain the apparatus for testing, sample preparation, and steps involved in the determination of the splitting tensile strength of rock and concrete specimens respectively by diametral line compression of a disk-shaped specimen [50,51]. The value of the tensile strength and tensile strain can be determined by the following equations:

$$\sigma_t = \frac{2P}{\pi Dt} \tag{4}$$

$$\varepsilon_t = \frac{d}{D} \tag{5}$$

where P is the tensile load, D, t and d are the diameter, thickness and vertical displacement of the sample respectively.

Meanwhile, the Young's modulus which is measured from the gradient of the initial straight line part of the tensile stress-tensile strain plot (Hibbeler and Fan) can be expressed as [52]:

$$E = \frac{\sigma}{\varepsilon} \tag{6}$$

Moreover, in order to obtain an acceptable consistency level in the results and to ensure agreement with theories of brittle failure relative to the sample size effects, Kumar and Prashanth and Sandoval et al. proposed that the ratio between the thickness and diameter t/D of the ceramic disk must be maintained within a range of 0.2–0.25 so as to ensure that fracture is triggered by tensile stress only [54,55]. It is also important to note that the t/D ratio above must fall within the range (0.2–0.75) highlighted in the ASTM D3967 and ASTM C496/C496M standards. Similarly, it is important to ensure uniform distribution of the load and decrease the friction between the sample and platen to a bearable level. With respect to this, usage of padding materials and lubricant paste have been proposed by Sandoval et al. and Fahad [56,57].

The typical fracture patterns exhibited by the broken ceramic samples are as follows: Triple-cleft fracture (TCF) [55,58]: This is typified by a central fissure running along the diametral axis of the point of load application (diametral fracture, DF) alongside secondary cracks that spread parallel to the central fissure and causes triple fragmentation due to the additional failure of the internal fragments. Load region fracture (LRF) takes place between the ceramic sample and compression platens. It consists of the presence of shear prism at generator culminating with tiny flakes from the disk detached from the sample surface adjoining the contacting platen. Moreover, total fragmentation of the ceramic sample can take place in severe cases such as in the combination of DF and LRF. The typical fracture patterns observed in porous ceramic materials are presented in Fig. 7.

3.2.2. Compressive strength test for porous ceramic composites

There are existing ASTM standards including ASTM C1424 and ASTM C365/C365M for testing monotonic compressive strength of advanced ceramics at room temperature and for compressive properties of sandwich cores respectively [59,60]. However, owing to some limitations in this category of advanced ceramics (i.e., porous ceramic composites), alternative test configurations may be followed [61]. Dam et al. presented a deformation-mode map for open cell alumina where the compressive strength was measured by obtaining from the compressive stress-strain graph the point of maximum load before the commencement of strong crushing of the sample [62]. The compressive strength and strain can be obtained by dividing the applied load by the surface area of sample and dividing the applied displacement by the sample thickness respectively according to the equations below:

$$\sigma_c = \frac{4P}{\pi D^2} \tag{7}$$

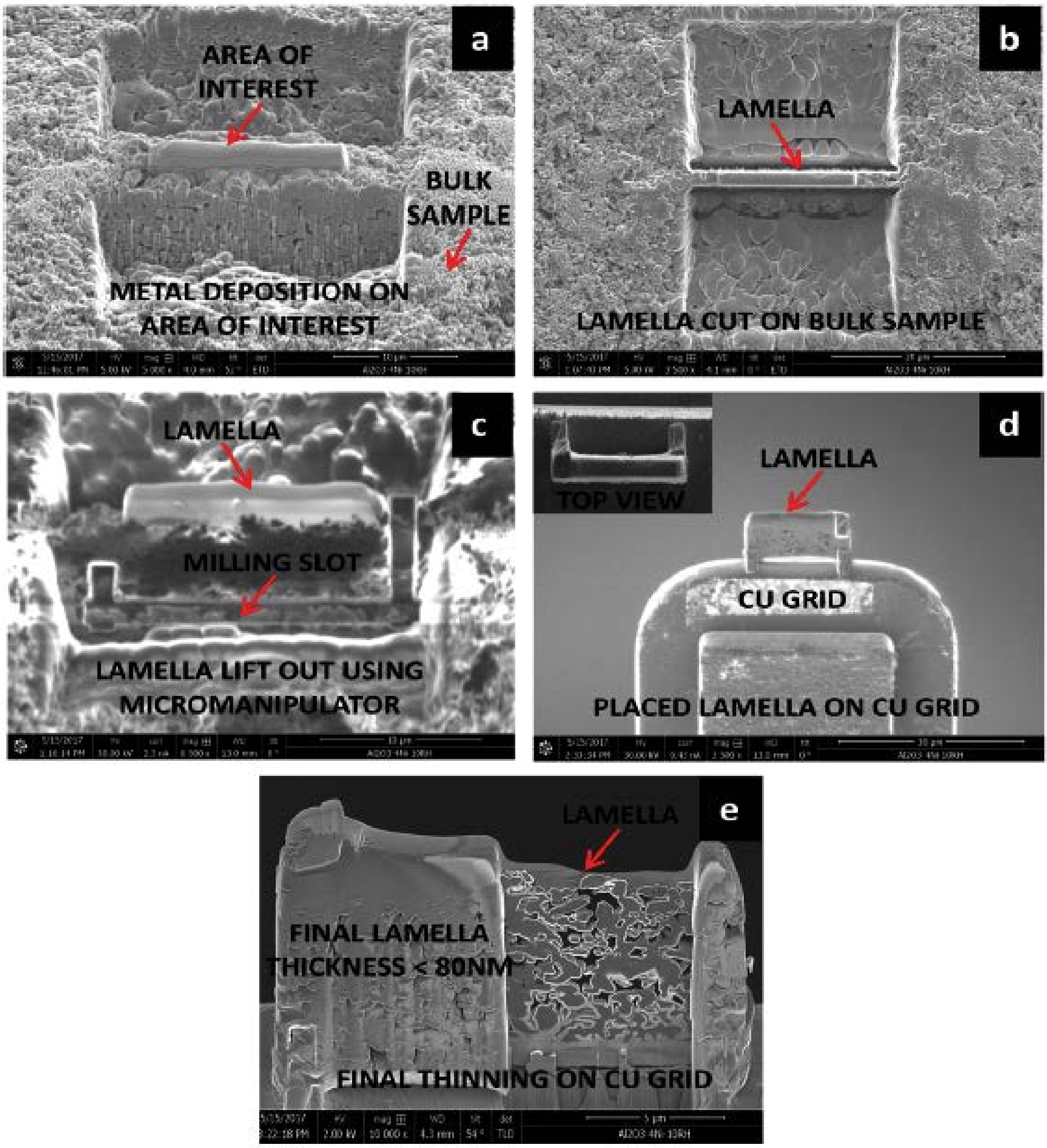

Fig. 4. Dual beam specimen preparation for TEM examination of porous ceramic composites: (a) metal deposition on area of interest, (b) lamella cut on bulk sample, (c) lamella lift out, (d) lamella placement on copper (Cu) grid, and (e) final thinning on copper grid [47].

$$\varepsilon_c = \frac{d}{t} \tag{8}$$

where P is the load (N), D and t are the diameter (m) and the thickness (m) of the disk respectively, and d is the actuator displacement (m).

3.2.3. Hardness test for porous ceramic composites

The measurement of hardness is an important testing procedure that has been utilized in several decades down the line by for measuring the level of resistance of porous ceramic composites to frictional forces such as abrasion. The ASTM standard, ASTM C1327 is frequently used as the standard test procedure for Vickers indentation hardness of advanced ceramics [63]. The value of the hardness (HV number) can be determined using the equation below:

$$\mathrm{HV} = \frac{1.8544F}{d^2} \tag{9}$$

where F represents the applied load (N) and d indicates the average length (m) of the two diagonals left by the indenter.

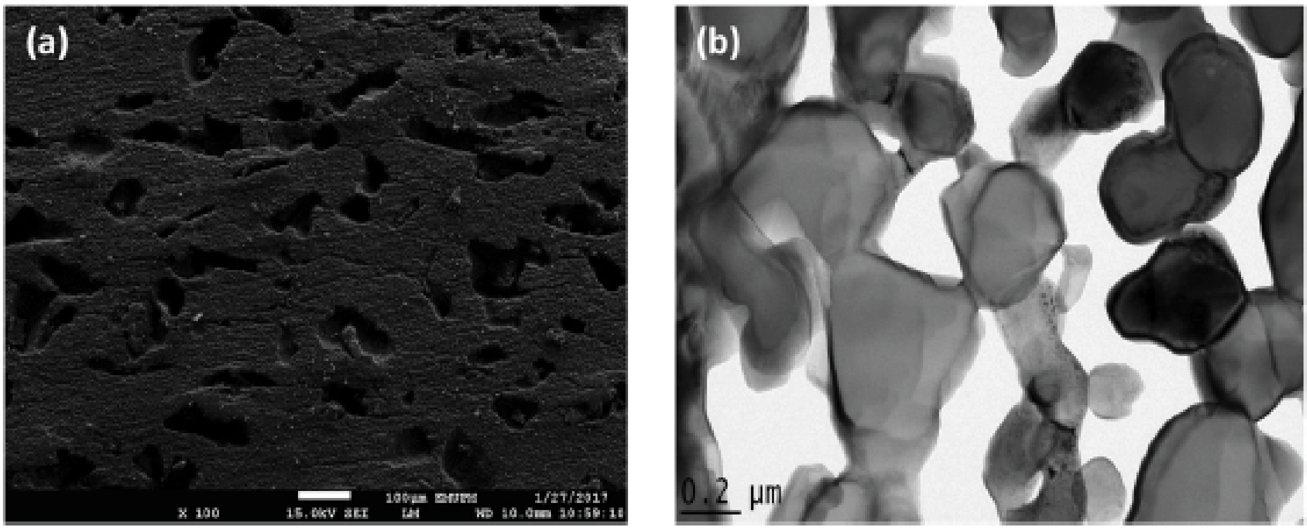

Fig. 5. (a) SEM micrograph for pore microstructure, and (b) TEM micrograph for granular microstructure of rice husk-shaped Ni-reinforced porous alumina composite [47].

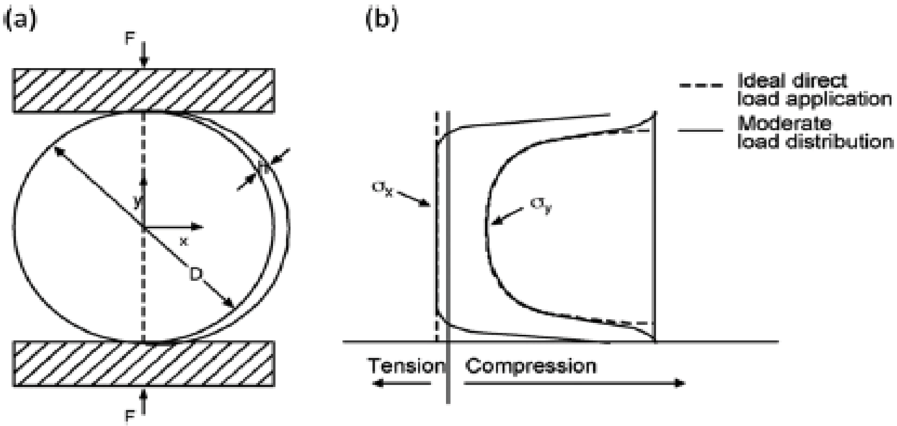

Fig. 6. Brazilian disk test (a) experimental device with direct load application and (b) stress distribution along the vertical plane [53].


Triple cleft fracture
Diametral fracture
Diametral fracture + Load region fracture
Load region fracture

Fig. 7. Typical fracture patterns observed in the porous alumina ceramics.

3.2.4. Flexural strength test for porous ceramic composites

The investigation of flexural strength is another test to evaluate the mechanical strength that has been utilized over the years to measure the capacity of bending strength of porous ceramic composites. ASTM C1674 explains the test set-up, sample preparation and steps to measure the flexural strength of advanced ceramics with engineered porosity (honeycomb cellular channels) at room temperature [64]. There are other ASTM standards such as ASTM C1161 and ASTM C1684 for room temperature testing of the flexural strength of advanced ceramics having rectangular and cylindrical geometries respectively [65,66]. The test can be conducted by utilizing both the four-point-1/4 point and three point loadings with prescribed spans and sample geometries as stated in the ASTM standards (Fig. 8).

For rectangular shaped porous ceramic composite samples, the formulas for the flexural strength in four-point-1/4 point flexure and three-point flexure are;

Four-point-1/4 point flexure:

$$\sigma_f = \frac{3PL}{4bd^2} \tag{10}$$

Three-point flexure:

$$\sigma_f = \frac{3PL}{2bd^2} \tag{11}$$

For cylindrical shaped porous ceramic composite samples, the formula for the flexural strength in four-point-1/4 point flexure and three-point flexure are given by:

Four-point-1/4 point flexure:

$$\sigma_f = \frac{4PL}{\pi D^3} \tag{12}$$

Three-point flexure:

$$\sigma_f = \frac{8PL}{\pi D^3} \tag{13}$$

3.3. Corrosion resistance properties characterization of porous ceramic composites

Corrosion mechanism study of porous alumina ceramics under different acidic and alkaline conditions can be conducted using the weight loss measurement method (cf. Eq. 10) which is the preferred method for ceramic materials, since the dielectric nature of these materials makes them unsuitable for other corrosion testing methods. Before taking measurements, porous ceramic samples are machined and polished to obtain a geometry of 18.5 mm (D) × 4.5 mm (t). Thereafter, samples are cleaned ultrasonically in ethanol for 10 min to degrease and remove traces of oxidation film. After drying, weighed samples are immersed in strong H_2SO_4 (20 wt%) and NaOH (10 wt%) aqueous solutions according to GB/T 1970-96, (1996) standard. An electric hot plate is employed to keep the solution temperature at 110°C for intervals of 2, 4, 6 and 8 h.

$$M_{\text{loss}} = \frac{M_0 - M^1}{M_0} \times 100 \tag{14}$$

where M_{loss} denotes mass loss rate after acid (or alkali) corrosion, %; M_0 indicates the mass of sample prior to corrosion, g; M^1 represents the mass of sample after acid (or alkali) corrosion, g; M_{loss} = mass loss rate after acid (or alkali) corrosion, %; M_0 = mass of sample before corrosion, g; M^1 = mass of sample after acid (or alkali) corrosion, g.

At the end of each corrosion test, samples are removed from the experimental set up and ultrasonically rinsed for 15 min to remove residual test solution as well as loose corrosion products. After which samples are dried until a constant mass was obtained. Fig. 9 shows the FESEM micrographs of agro-waste-shaped Ni-reinforced porous alumina ceramic composites before and after corrosion in strong acid and alkali mediums.

4. Ceramic composites for water treatment

One of the most pressing challenges of the 21st century is water pollution, this is because water security have profound consequences on societal wellbeing and the survival of global economy [1,68,69]. The application of porous ceramics for water treatment to ensure availability of portable water have recently attracted remarkable interests. Porous ceramics are made of refractory oxides such as alumina, zirconia, titania and some other forms of oxides. Porous ceramics are often explored as a very suitable alternative and are advantageous compared to other water treatment materials due to their chemical, thermal and structural stabilities and are preferred treatment material because they do not distort operational process, they are known to have resistance to high temperature and long treatment life span which implies that they are cost effective materials for water treatment. In general context, most pathogenic microorganism and pollutants can

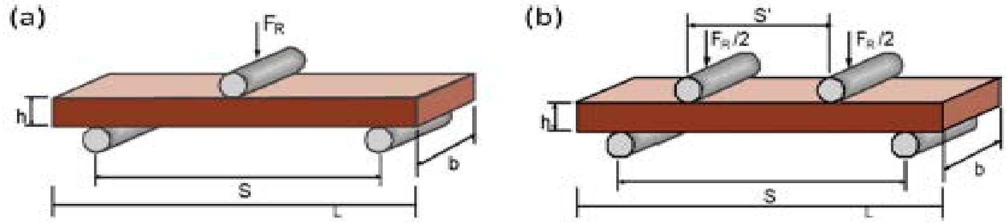

Fig. 8. Schematic representation of the experimental (a) three-point flexure and (b) four-point flexure [53].

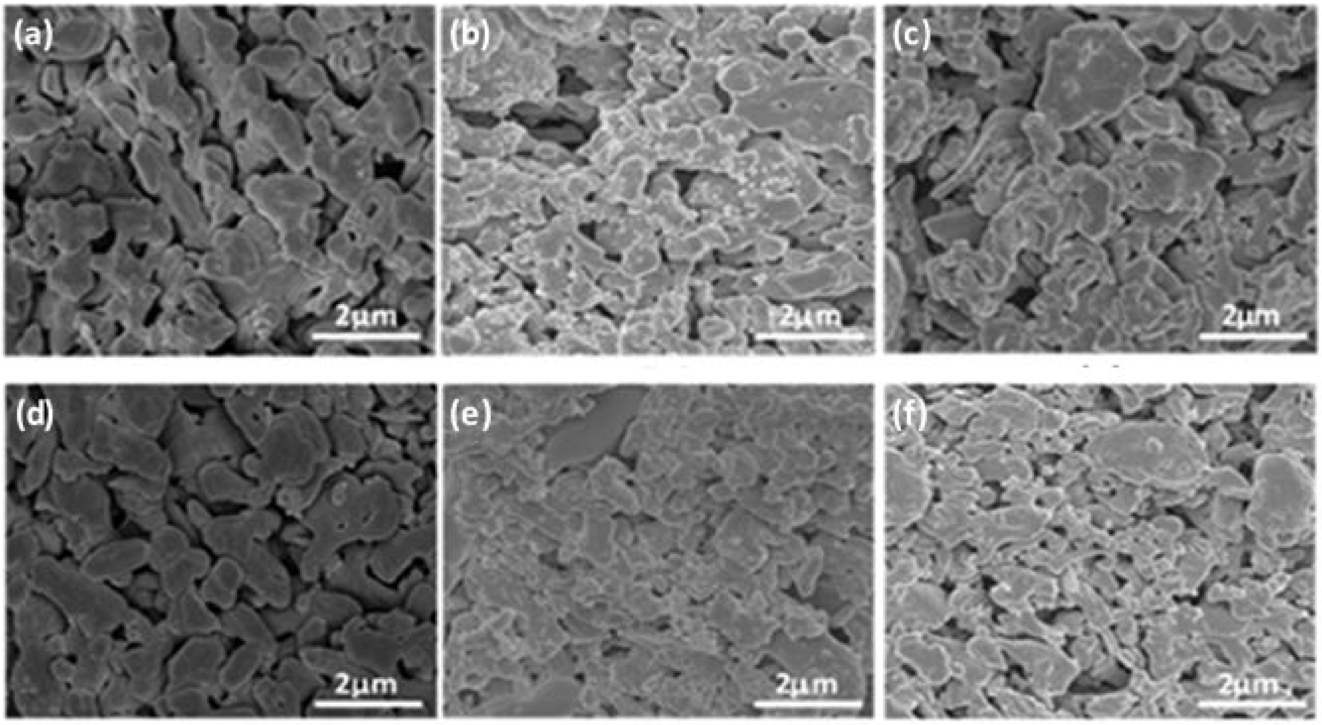

Fig. 9. FESEM micrographs of RH-graded Ni-reinforced porous alumina ceramics composites after corrosion for 8 h under different conditions (a) un-corroded, (b) 10 wt% NaOH, (c) 20 wt% H_2SO_4, and, SCB-graded Ni-reinforced porous alumina ceramics composites after corrosion for 8 h under different conditions (a) un-corroded, (b) 10 wt% NaOH, (c) 20 wt% H_2SO_4 [67].

be trapped on the surface of porous ceramics, however the effect of the surface attachment alone cannot satisfactorily distort the growth of microorganisms which can result to resistance to antimicrobial treatment. This drawback can be overcome by coating the ceramic surface with nanomaterial such as silver nanoparticles. Silver nanoparticles have better prospect as an antibacterial coating due to morphologies that allows the control of released silver [70]. However, if adsorption occurs on a surface of porous ceramic that exhibits weak force of attraction such as vanderwaals, there is the tendency for a wash away to occur by the momentum when water flows through the porous ceramics resulting in the dispersal into the liquid medium.

4.1. Activated alumina

The intrinsic characteristics of activated alumina encourages adsorption of pollutants on its surface. Lin et al. [71] stated that activated alumina is better suited for the adsorption of heavy metals compared to membrane separation and ion exchange process. Mor et al. [72] reported that the significance of operating parameters including pH, contact time, adsorbent dosage and initial concentration influenced the sorption capacity of activated alumina for the removal of Cr ions. The authors attributed the effect of pH towards the increase in uptake capacity to the decrease in the electrostatic interaction involving negatively charged Cr ions and positively charged surface of the adsorbent. Naiya et al. [73] investigated the adsorption capacity of activated alumina for the removal of Cd and Pb ions from aqueous solution and suggested that both adsorption and precipitation process occurred on the surface of the adsorbent as the pH increases. Ji et al. [74] reported the removal of Se (VI) and Se (IV) from activated alumina in a batch and continuous flow reactor and revealed that the adsorption capacity of activated alumina was achieved within 12 h equilibrium time. Although the effect of $NaHCO_3$ concentrations adversely affected the adsorption of Se (VI) on the membrane adsorbent.

4.2. Mineral based alumina ceramic composites

Alumina-based adsorbents have been given considerable attention for pollutant remediation due to their low economic cost of materials, effective removal of pollutants and they are environmentally friendly. Ceramic membranes have unique properties and the capacity to withstand extreme backwashing and aggressive chemical cleaning including effective regeneration potentials during application [75,76]. However, commercialized ceramic membranes utilize very expensive ceramic materials, such as alumina, titania and silicon carbide to ensure purity. The potentials of ceramic composite such as alumina ceramic composite for wastewater treatment is attributed to the abundance of the natural minerals and the remarkable lower sintering cost. The synthesis of pyrophyllite-alumina ceramic composite for the treatment of domestic wastewater demonstrated cost effective approach and alternative membrane treatment method. Pyrophyllite is a natural clay material predominantly in South Korea. It serves as an alternative to low-cost ceramic membranes. Pyrophyllites have a composition consisting of aluminium silicate hydroxide ($Al_2Si_4O10·(OH)_2$) containing one mole of aluminum(III) oxide (Al_2O_3) and four moles of silicon dioxide (SiO_2). Although the flexural strength of mineral based pyrophyllite as support layers may not adequately provide the needed sufficiency, it could serve as a support material with the addition of alumina for the enhancement of composite. However, even though pyrophyllite is an environmentally promising new material, the problem of permeability is a major issue for microfiltration. [77] added diatomite for the enhancement of its permeability. Hence, a diatomite-kaolin composite was formed, while diatomite served as the matrix, kaolin served as a strength enhancer. Meanwhile, pyrophyllite served as the matrix in the formation of pyrophyllite-diatomite composite [78], while diatomite as a pore former. According to findings, an alumina-coated pyrophyllite-diatomite composite support layer could be reliably maintained during the microfiltration test [79,80]. This implies that the low cost natural minerals exhibits water permeability which can be utilized as an effective filtration membrane and a cost effective alternative to conventional high cost porous ceramic membranes. The fabrication of low cost fly ash alumina composite has been reported to be an alternative cost effective membrane for wastewater treatment. However, the challenge of broad particle size of materials such as fly ash (1–100 μm) could adversely affect the efficiency of the ceramic membrane in terms of separation of pollutants during wastewater treatment [81–83]. This drawback can be eliminated by fabricating a membrane of smaller pore size diameter, additionally to ensure effective separation accuracy, there is need for the requirement of coating and sintering of the intermediate support layers [84] (Rashad et al., 2020). In this context, to reduce cost of fabrication of membrane and the number of intermediate layers on a macroporous support, Zhu et al. [85] fabricated fly ash/ alumina composite membrane having a pore size by thermal spraying process. The membrane layer was coated without intermediate layers on a macroporous fly ash. This process reduced fabrication cost since there was no coating of many intermediate layers, the process can be considered for environment preservation by enabling the recycling of fly ash waste. The performance of the synthesized fly ash alumina ceramic composite was investigated for the separation of oily emulsion from tin wastewater. Studies have found that the valorization of drinking water sludge can notably be applicable in ceramics due to the enhancement of mechanical strength as a result of partial replacement of clay with sludge. Mouratib et al. [86] synthesized drinking water sludge membrane predominantly consisting of alumina as a ceramic membrane through dry pressing and sintering. The performance of the alumina ceramic membrane was applied for the removal of suspension in synthetic and industrial wastewater.

4.2.1. Ceramic carbonaceous composites

The application of silicon oxycarbide ceramics for water purification is gaining much attention. Silicon oxycarbide ceramics composite comprises of Si–O–C tetrahedral. The covalence of C and O exists as Si–O–C with Si atom in the amorphous phase [87]. The surface composition and chemical functionality of the carbonaceous microspheres, precursor composites and pyrolysis revealed that the distribution of C spheres occur outside the silicon oxycarbide ceramics. Coal waste and ashes from thermal power station are examples of ceramic raw materials for the production of composites [88]. The fabrication of carbonized silk ceramic composite via one step firing process indicated good cyclic property with homogenous heat distribution is shown in Fig. 10 [89].

Carbonaceous material such as carbon nanotubes (CNT), carbon nanodots including graphene oxide have been incorporated for the improvement of the water permeability of designed composite membrane due to its chemical, thermal stability and also its antifouling properties. The essential feature of ensuring selective water permeability by tuning structural defects makes it a favourable membrane for selective water treatment [90]. CNTs are nanostructured one-dimensional carbon materials and is attracting immense interest because of their intrinsic physical and chemical characteristics [91,92]. CNTs-based filters are of remarkable interest for water purification [93], this includes the removal of hydrocarbons from petrochemical wastes due to its potential and capacity for oil and water separation in a separation membrane [94,95]. This property can be attributed to their affinity for hydrophobic solutes as a result of their CH/π-interactions. A thermally resistant mullite-CNT composite for the removal of oil droplets from emulsions was investigated by Zhu et al. [85]. The composite material comprising of hierarchical structures was studied for the removal of tiny oil droplets from oil in water emulsions at high temperature.

From the morphology study, it was observed that the mullite-CNT composite has a characteristic membrane structure with the propensity for highly porous interlaced CNT thin layer which includes macro-void finger-like layers having CNTs grown along the macro-channels. Due to the porosity and interlocking behaviour of the high flux membrane, mullite CNT composite which permits low operating pressure enhanced the separation of oil in water emulsions at high-temperature to produce hot water without the need for precooling. Carbonaceous materials are widely used interfacial membranes for water treatment. A low cost biochar based clay composite ceramic filter for point of use water treatment was reported by Chaukura et al. [96]. The fabrication of the ceramic filter was achieved via traditional firing method using a predetermined mixture of dry clay powder, sawdust and distilled water which were mixed to obtain a thick dough. The synthesized porous ceramic composite filter exhibited surface roughness both internally and externally which is significant for hydrophilic interaction and water transport [97]. Hydrophilic membranes effectively remove hydrophobic solutes from analyte and decreases the tendency for fouling [98]. The carbon ceramic composite effectively reduced the concentration of TDS and DOC in the filtrate, although there was evidence of increase in the pH of the permeate which could be attributed to the effect of leaching of alkaline and alkaline earth metal oxides such as CaO K_2O, Na_2O from the ceramic [99]. The efficiency of the carbonaceous ceramic composite was as a result of the active functional groups on the surface of the biochar [100]. Acidic functional groups

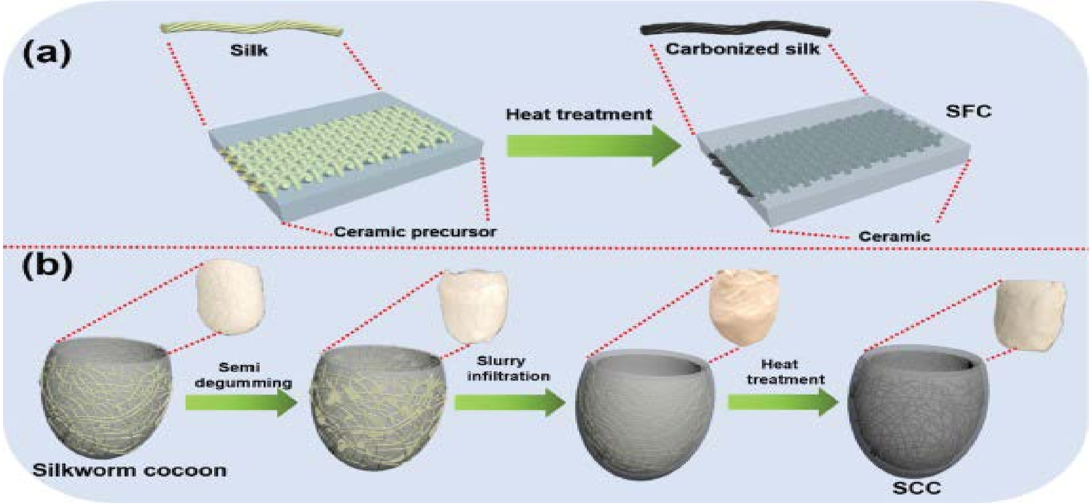

Fig. 10. Scheme of the fabrication process of (a) silk fabric based composite (SFC) and (b) silkworm cocoon based composite (SCC) [89].

such as carboxylic, carbonyl, lactonic and phenolic groups on the surface of biochar via chemical oxidation has the capacity for the adsorption of pollutants from wastewater.

The removal mechanism of pollutants from wastewater via a carbonaceous ceramic composite depends on the chemical composition on the active sites. The synergistic effect in the liquid phase of fluxes such as alkali and alkaline earth metals at a relatively low temperature in the formation of the internal structure is a subject for intensive research.

4.2.2. Silica based ceramic composites

Silica based ceramic composite derived from natural materials such as waste from rice husk for water treatment is gaining attention. These materials are low cost with high selectivity and chemical stability [101]. However, silica ceramic composite have limited application for water treatment compared to alumina based ceramic composite. This is attributed to the interaction of Si–O–Si bonds that exists in the silica structure with water molecules which can result to the formation of Si–OH hydroxyl groups, resulting in the damage of the pore structure of the silica membrane [102]. Therefore there is the need for the enhancement of its hydro stability. For the modification of surface properties of silica ceramic materials, incorporating methyl groups in silica microstructure can improve on the stability of hydrophobic silica based membranes. Panchal et al. [103] have reported the improvement of silica ceramic composite using activated carbon eggshells nanoparticle. The strong intermolecular bonding between silica, activated carbon and eggshell nanoparticle was attributed to the formation of the porous surface of the composite which influenced the filtration process as indicated in Fig. 11.

At high temperature and under humid condition, it has been reported that silica based composite prepared by sol–gel methods with the combination of inorganic oxides such as alumina (SiO_2) and zirconia (ZrO_2) improves the thermal stability of silica membranes [105].

The interaction between SiO_2 and Al_2O_3 of the ceramic during sintering has been reported to improve on the chemical and mechanical stability of the ceramic composite [106]. In addition, for the reduction of sintering temperature of the ceramic composite, oxides of alkali and alkaline earth metals can serve as flux agent [107]. To optimize the performance of silica ceramic composite, mitigation of membrane fouling is very important. Fouling occurs as a result of resistance attributed to the formation of cake-like layer on the surface of the composite membrane thereby reducing the efficiency of the membrane for clear water filtration. To achieve the purpose of anti-fouling behaviour, Alias et al. [108] reported the analysis of the permeation of water flux from polysulfone–rice husk silica ash mixed-matrix composite membranes using PI membrane and suggested that the hydrophilic rice husk ash additive exhibited a uniform finger-like sub-layer which can be attributed to the enhancement of the performance of anti-fouling characteristics of the composite.

4.2.3. Titanium ceramic composites

In the field of water purification, separation including photocatalytic degradation of toxins, titanium dioxide (TiO_2), has been widely applied for pollutants remediation to ensure environmental safety. However, the drawback of TiO_2 in wastewater treatment is attributed to its narrow band gap consisting of 3.2 eV anatase which only allows a permissible ultraviolet (UV) light less than 387 nm. Therefore to ensure improvement and structural stability of TiO_2, research on the synthesis of composite containing titania has been reported [109].

The biocompatibility of titania including its mechanical strength is attributable to its outer oxidized layer. Incorporating titania-based active layer into porous ceramic membranes is assumed to have potential to enhance improved separation performances in the field of membrane technology and separation processes which includes microfiltration (MF), ultrafiltration (UF) and nanofiltration (NF) [110]. The surface morphology of ceramic composite coated on titanium by micro arc oxidation (MAO) is illustrated in Fig. 12.

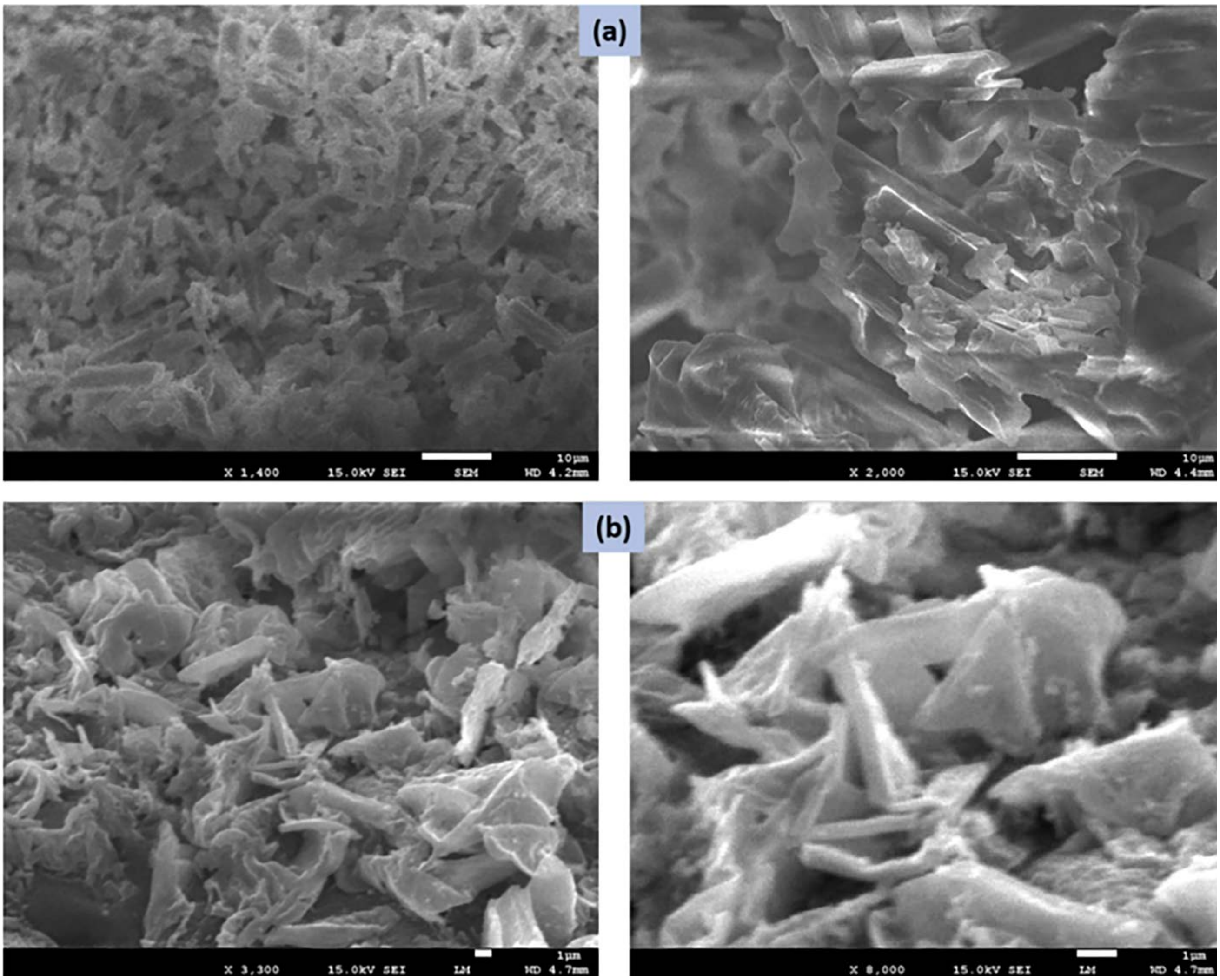

Fig. 11. Morphology of silica activated carbon-eggshell nanoparticle composite [104].

A non-uniform porous layer consisting of average pore size from 0.5 to 2.5 μm was observed on the surface of micro arc oxidized (MAO) coated surface of the composite (Fig. 12a). These micro pores could be attributed to the formation of gas bubbles exhibited by the material in the molten phase. However the incorporation of SiC and SiO_2 decreased the porosity of the composite membrane suggesting that the micro pore size is proportional to the coating process. Zhang et al. [112] have stated that the addition of SiC influences improved oxidation resistance by promoting the formation of a silica-rich ceramic membrane. Mohsenifa et al. [113] reported that increase in the concentration of ceramic titanium oxide particles in coating influences increase in ionic absorption. The surface morphological changes of ceramic composite occur with the addition of titanium oxide particles and could result to the transformation of the composite membrane from a non-uniform grains membrane surface course to a smooth surface and fine grains membrane surface with enhance porous structure for the attachment of pollutants from wastewater. Sun et al. [114] fabricated a composite membrane by depositing TiO_2 particles on ceramic substrate. The photocatalytic properties of TiO_2 indicated its homogenous dispersion on the substrate which by absorbing the photons passing the TiO_2 layer influenced the photocatalytic degradation of organic dyes. This suggested that improvement of photon utilization for the degradation of organic dye pollutants could be enhanced on a ceramic substrate.

4.2.4. *Zirconia oxide ceramic composite*

Zirconium dioxide (ZrO_2) is a metal oxide with high surface area, making it a good adsorbent for water and wastewater treatment especially for oil-water separation. The potential of ZrO_2 includes its non-toxicity and ease of production. However, the pore size and surface area of ZrO_2 depends on the thermal stability of the material [115]. Zirconia materials treated at elevated temperature will result to reduction in surface area which may be attributed to decrease in the stability of zirconia as the temperature increased [116]. The stability rate was found to decrease from 100% to 75.2% indicating that elevated

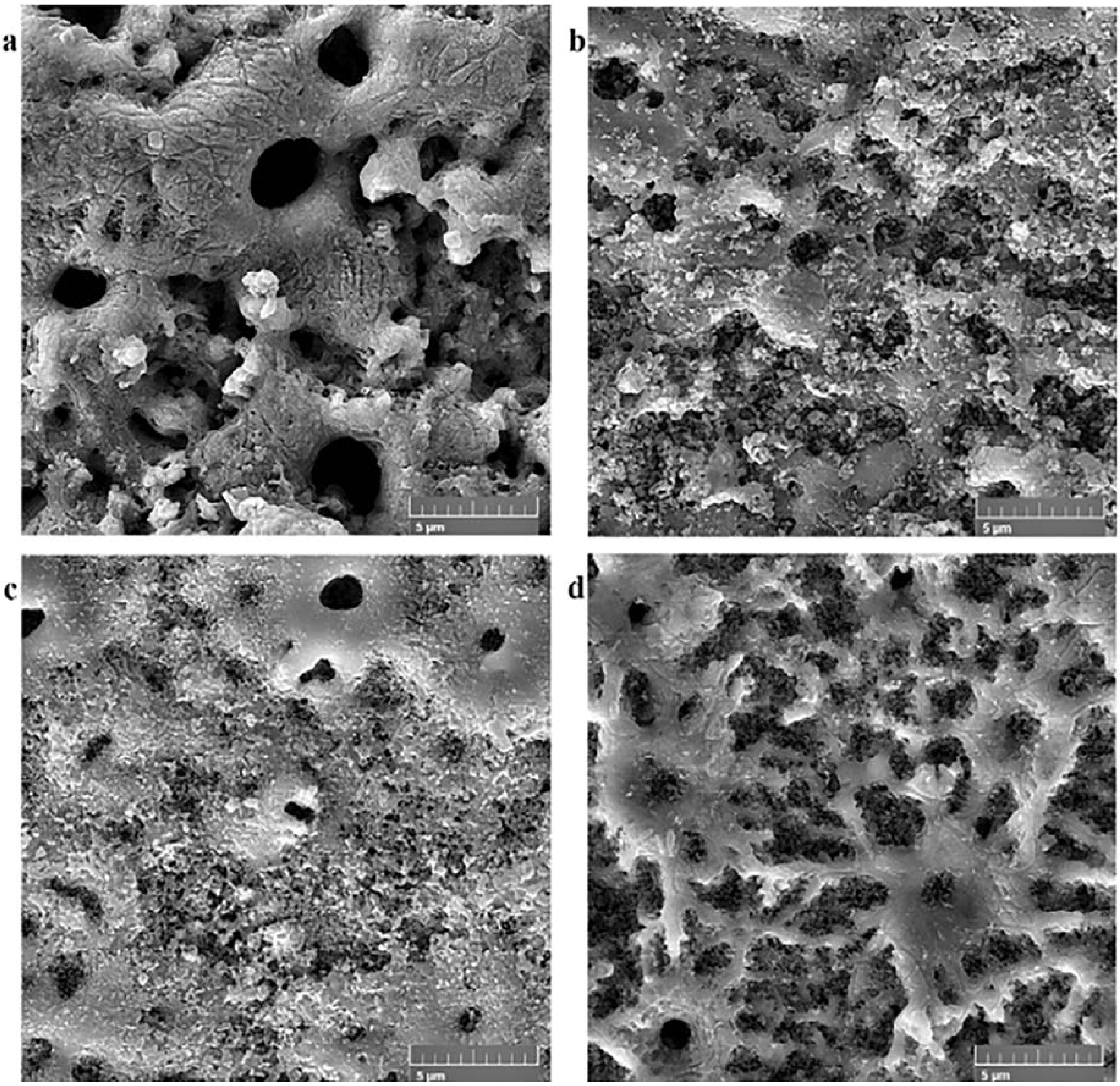

Fig. 12. Surface morphology of (a) M.A.O coated ceramic composite membrane, (b) M.A.O coated ceramic composite membrane + SiC, (c) M.A.O coated ceramic composite membrane + SiO_2 and (d) M.A.O coated ceramic composite membrane + E.Ph + SiC membrane [111].

temperature plays a significant role in the stability and phase transition of zirconia in composite. Increasing the temperature will continue to decrease the surface area of the material. Fakeeha et al. [117] reported that at increased calcination temperature (600°C to 800°C) there was a remarkable decrease in the surface area and the pore volume although with increase in pore diameter. Zirconia di oxide based ceramic composite is very valuable for the microfiltration, ultrafiltration of oily wastewater and for the removal of organic matters in a post treatment refinery processes. For the removal of organic pollutants from water, Boussemghoune et al. [118] synthesized a tubular zirconia membrane on a ceramic support using kaolin powders for the preparation of the membrane support. Inorganic and organic additives used for the preparation of the support were $CaCO_3$ and Methocel respectively. This was followed by a filtration test via a tangential filtration system. The surface morphology of the composite membrane is illustrated in Fig. 13.

The synthesized zirconia ceramic composite membrane indicated a decrease in the permeate flux of raw drinking water during the first 20 min after which it became constant. This could be attributed to the deposition of suspended matter on the surface of the membrane, the filtration system

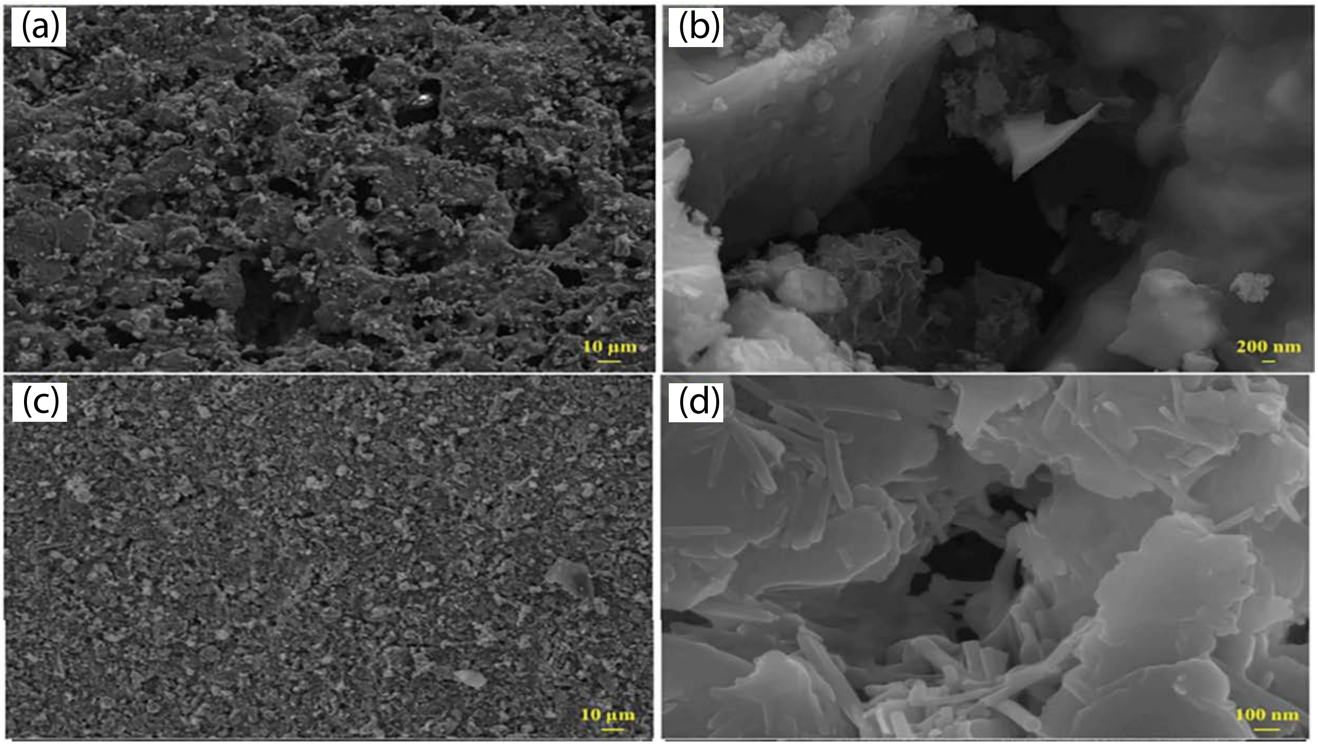

Fig. 13. SEM images indicating support and ceramic membrane (a,b): the outer surface of the support material; (c,d): the inner surface of the ceramic composite membrane [118].

indicated a significant improved permeate for turbidity and phosphate removal compared to the raw water. Similarly, the permeate contained zero number of coliforms which signified the efficiency of the zirconia based ceramic composite. He et al. [25] have reported that the hydrophilic properties of zirconia results to high flux, low fouling and high thermal resistance during water treatment.

4.2.5. Zeolite based ceramic composite

The interest of zeolitic membrane have shown intense growth over the last two decades. This is due to its unique configuration and pore structures due to the tendency for the alteration of the pore size of the membrane as a separation layer. In addition, the functional groups on the zeolitic structure can alter the surface property which includes the hydrophobic/hydrophilic behaviour of the material. Zeolites are very effective adsorbent for sorption and ion exchange in wastewater treatment. However, the application of zeolite in different technological processes is relatively connected to their physical-chemical properties attributed to their geological deposits [119]. To explore the compatibility of liquid phase separation in a hydrothermal treatment process, zeolitic membranes were synthesized on low cost ceramic support. Fig. 14a–d illustrate the surface morphology via SEM images of ceramic support including zeolite composite membranes (MCM-41, MCM-48 and Faujusite (FAU)) [120].

In Fig. 14a, reduction in the zeolitic pores can be attributed to small microporous channels which are subjected to diffusional limitations [121,122], compared to the ceramic support especially cubical FAU formed in Fig. 14d. Synthesis of zeolite composite consisting of considerable intracrystalline mesoporous surface can facilitate better diffusion transport channel [123]. As shown in Fig. 14b–d, more pore structures were formed as the sintering temperature increased. The separation of Cr (VI) gives an indication of promising permeate flux when FAU zeolite was deposited on the ceramic support. The result can be attributed to the compatibility of the separation of the liquid phase and the hydrophilic behaviour of the FAU zeolite membrane despite the pore size of FAU zeolite membrane compared to MCM-41 composite membrane.

Jiang et al. [124] prepared a silicon carbide ceramic composite membrane using zeolite residues via sintering in air atmosphere and investigated the effectiveness of the ceramic composite in terms of permeance of the membrane for separation of oil and water recovery. A complete oxidation of the activated carbon resulting in formation and emission of CO_2 at 600°C to form pores in the SiC ceramic membrane was noticed. The produced SiC composite membrane demonstrated high water permeance of 3,700 L/ m^2/h bar and porosity of 46%, which was attributed to the more than 90% rate of oil rejection of oil achieved.

Zeolite based ceramic composite membrane indicated high prospect for the separation of oil and water recovery from wastewater. However, for technology transfer from laboratory to industrial practice towards oil separation and recovery, the method of synthesis or additional of additives that have the potential of decreasing the sintering temperature is required. In this context, future works that improves on the synthesis of zeolite ceramic composite membrane will

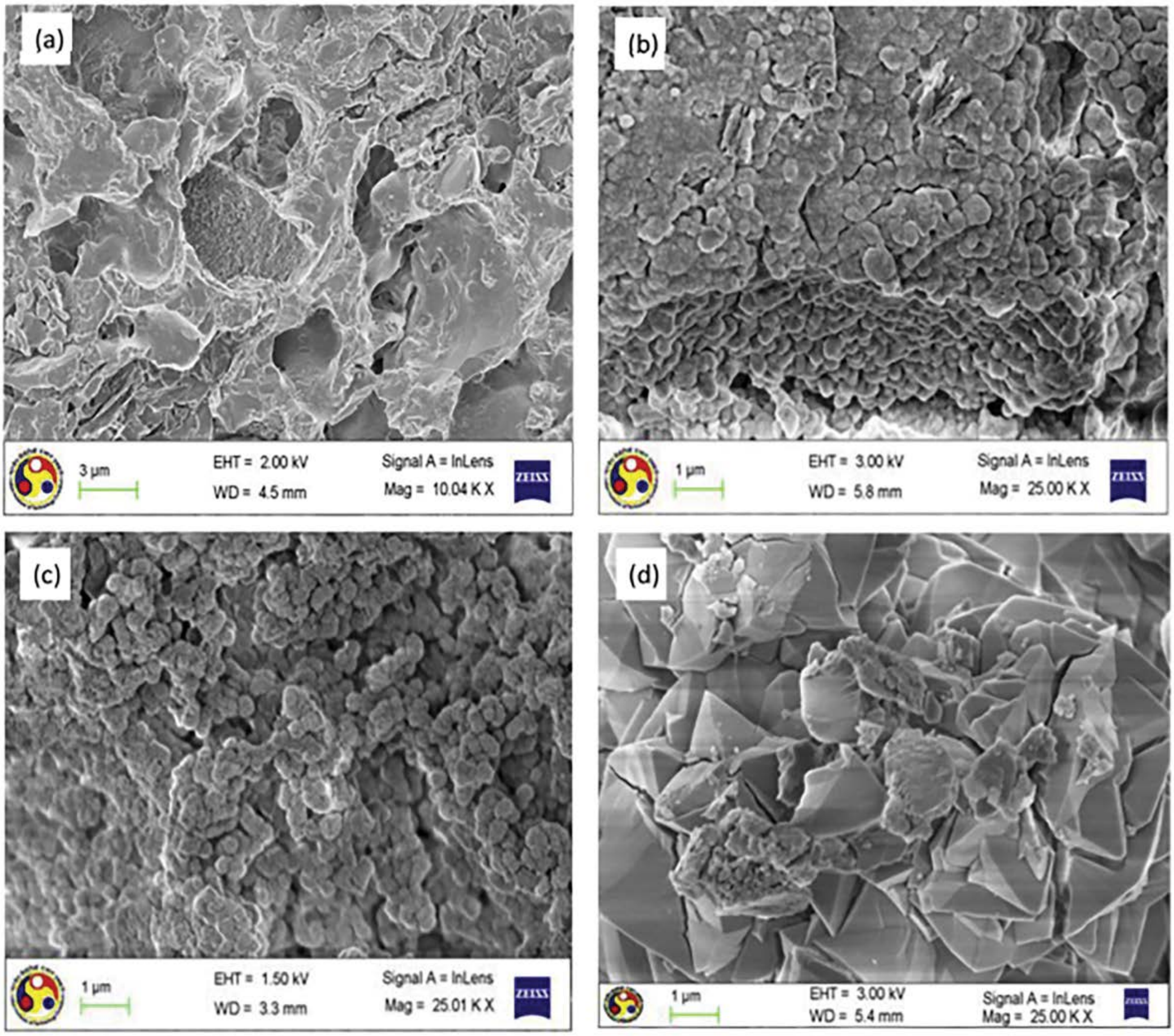

Fig. 14. SEM images of (a) ceramic support, (b) MCM-41, (c) MCM-48, and (d) FAU ceramic composite membrane [120].

enhance operational efficiency of the membrane for water and wastewater treatment.

Ceramic membrane water filters have exhibited effective treatment efficiency for the removal of pollutants from water and wastewater. The improvement of the removal capacity can be enhanced by fabricating ceramic composite including oyster shells powder in the composite formulation [125]. A biologically aerated filter media can be fabricated using oyster shell based ceramic composite for the treatment of municipal wastewater.

4.3. Oyster shell ceramic composite

The utilization of wasted oyster shells has been explored as the contact media for the purification of domestic wastewater [126]. The authors fabricated a three horizontal flow tank treatment system consisting of horizontal flow and aerated oyster shell tank, horizontal flow oyster shell tank, and horizontal flow gravel tank. It was revealed that the horizontal flow and aerated oyster shell tank exhibited effective removal capacity of BOD_5, SS, NH_4–N, NO_3–N, PO_4–P and TP compared to the other treatment systems. It was concluded that oyster shells demonstrated better water removal capacity of the pollutants as a suitable material for the subsurface flow compared to the use of gravels. Oyster shell powder in matrix has been reported to improve the denitrification performance in upflow packed bed bioreactors [127]. Yen et al. [128] have also revealed that oyster shells or ceramic can be combined as bio-media for the degradation of organic matter in water due to the support layers of oyster shells which enables a biofilm with the release of $CaCO_3$. Hence, oyster shell can form as essential component of composite membrane for water purification and wastewater treatment. Oyster shell can be utilized for the improvement of pore networks in membrane structure. Deutou et al. [129] have synthesized highly porous anorthite ceramic membrane by incorporating oyster shells powder. The production of nano and meso size intergranular pores was attributed to the crystallization of gehlenite and anorthite by CaO produced by the calcined oyster shells at low temperature. Fig. 15 illustrates a micrograph of the porous membranes with addition of 10 wt.% of calcined oyster shell to membrane structure at 1,200°C (Fig. 15a–c) and 1,300°C (Fig. 15d–f).

The surface morphology in Fig. 15 indicated that the pores size of the membrane at 1,300°C. It was revealed from the morphological properties in Fig. 15d–f were larger compared to those at 1,200°C (Fig. 15a–c). Therefore, it implies that the change in pore structure have close linkage to the CaO–Al_2O_3–SiO_2 system liquid phase. The incorporation of oyster shell powder in the matrix networks at lower sintering temperature reduced the cracks and defects which indicated good quality of the membrane.

5. Challenges and prospects of porous ceramic composites

The issues associated with fouling of membrane is a major constraint limiting the application of membranes for water purification and wastewater treatment, the problem is attributed to salinity of membranes. This challenge is majorly as a result of pore size of membrane, porosity, pore distribution including membrane surface charge, pH and ionic strength. However, effective pre-filtration process for the removal of large molecules could reduce fouling of the membrane since larger particles can affect the passage of smaller particles through the membrane. Fabrication techniques have a significant impact on the reduction of membrane fouling. The fabrication techniques and processing parameters are critical determinants to improve the quality of ceramic-based composite membranes for water and wastewater treatment. The optimization of operational parameters during processing could increase transmembrane pressure by maximizing flux at the same time reducing fouling of membrane, this includes the increase in cross-flow velocity. The mechanical properties of ceramic composite such as its inherent brittleness still could be further enhanced despite effective fabrication techniques. For example, the flexural strength of mineral based materials such as pyrophyllite as support layers may not adequately provide the needed effectiveness, it could serve as a support material with the addition of alumina for the enhancement of composite. However, even though pyrophyllite is an environmentally promising new material, the problem of permeability still remains a major issue for microfiltration. Ha et al. [130] have incorporated diatomite for the enhancement of its permeability resulting in the formation of diatomite-kaolin composite, while diatomite served as the matrix, kaolin served as the strength enhancer.

Over the years, several conventional treatment methods of wastewater pollutants have been reported in the literature, however with less impact in terms of treatment efficiency and low economic benefit for the treatment of effluent at low concentration. Some of the methods are reverse osmosis, solvent extraction, sedimentation, flotation, ion exchange, chemical precipitation, combined air flotation and membrane, aerated heterogeneous process advanced oxidation, coagulation–flocculation, mixed matrix adsorption and membrane process.

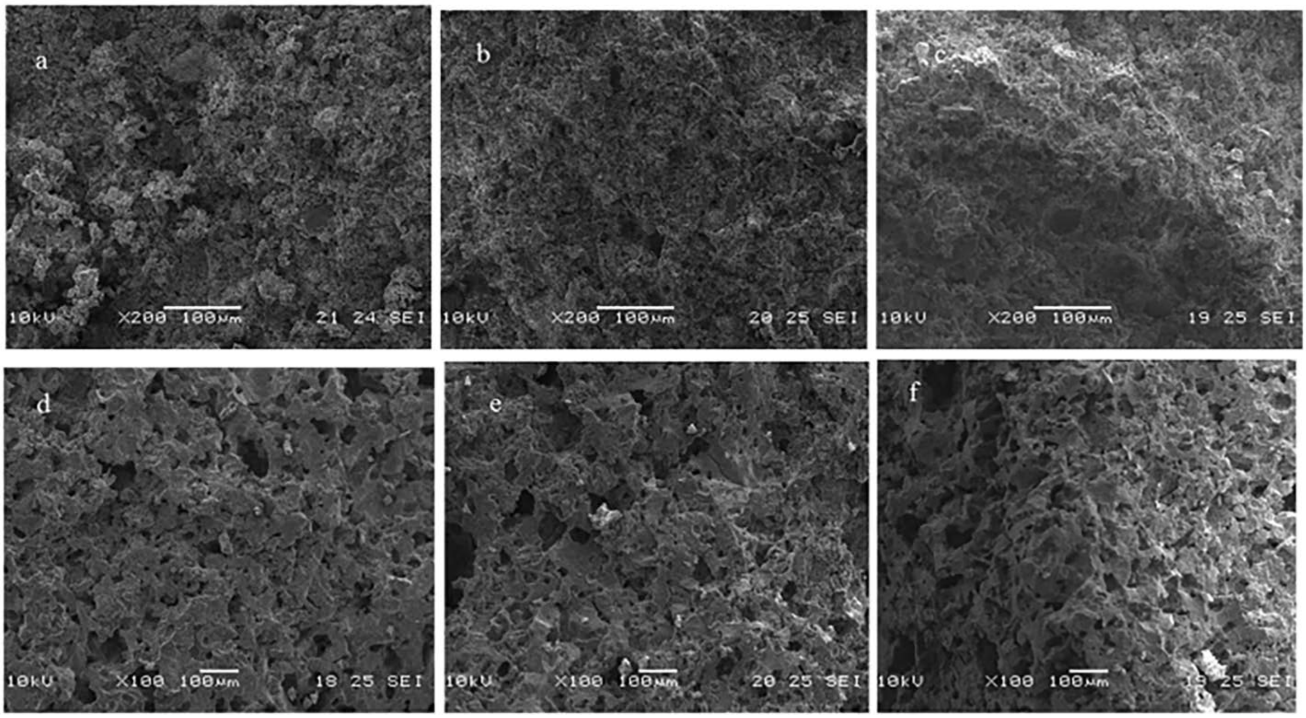

Fig. 15. Micrographs of the porous membranes with addition of 20 wt% of calcined oyster shell: phase transition at 1,200°C of different mass ratio, phase transition at 1,300°C of different mass ratio respectively [129].

Nowadays, low cost adsorbent have been extensively investigated as a replacement for commercial activated carbon with high treatment efficiency by adsorption [75]. However, with trend of advancement in the adsorption process, there are limitations to this method due to their small capacity and difficulty for large-scale application. Adsorbents are applied for wastewater treatment on the basis of their potential to adsorb priority pollutants in the wastewater and are often combined as composite material. Hydrophobic adsorbents have the propensity to adsorb non-polar solutes in aqueous solution while the adsorption of polar solutes in the adsorbate are mostly suitable on a hydrophilic surface. Recently, the application of ceramic composite membranes for the adsorption of recalcitrant hazardous pollutants have the potential of creating next-generation water purification media with high treatment efficiency which are reusable. The synthesis of ceramic composite membranes for membrane adsorption can be effective and can serve dual function of membrane filtration and adsorption for the removal of organic pollutants and heavy metals. The fabrication and application of ceramic composite membranes for the remediation of varieties of priority pollutants is significant because of their pore forming networks, thermal and chemical stability. For instance, a small amount of liquid phase in the sintering process of alumina ceramics can induce the anisotropic growth of alumina grains, while the brittleness of alumina ceramic materials can be greatly improved by forming a large number of rod-shaped crystals with a large aspect ratio in the alumina matrix. Similarly, the phase transition of zirconia is capable of promoting increased strength and toughness of the material. This characteristic of zirconia makes it a very suitable additive for strengthening and toughening in ceramic materials, thus capable of forming a series of zirconia toughening ceramics. Studies have shown that the addition of 5% SiC and 15% ZrO to the matrix of alumina is capable of improving the brittleness of alumina ceramic membrane. Ceramic membrane has advantage over other organic membranes currently used for industrial applications. This is due to its good chemical stability, good oxidation resistance, high abrasion resistance, high temperature resistance, narrow pore size distribution and high separation efficiency. This has made application of ceramic membrane an ideal material for the removal of pollutants from wide range of wastewater which includes municipal water treatment, oil and grease wastewater, sewage wastewater, textile wastewater and printing, greywater and dying wastewater [76,131]. The stability of ceramic-supported composite membranes is influenced by the degree of adhesion between the ceramic substrate and the functional layer [132]. The microstructure and functional characteristics including the method of fabrication determines the degree of adherence, compatibility and its sustainability for water and wastewater treatment.

6. Conclusion

This review extensively presents both low-cost and highly reliable processing techniques for developing porous ceramic composite membranes employed for water and wastewater treatment. Processing techniques such as pore-forming agent technique, vacuum impregnation process and 3D gel printing have been highlighted as viable techniques for tailoring the pore network and porosity of the developed porous ceramic composite membranes. Meanwhile, requisite standards with supporting studies on the characterization of microstructure, porosity, mechanical and corrosion resistance properties have been highlighted in this review. Efficient and simplified fabrication processes such as synthesis, coating and sintering have been demonstrated in this study. Improved properties, enhanced fabrication techniques and reduced production costs of ceramic composites membrane have been highlighted in this review towards removal of pollutants of water and wastewater. Although ceramic composites exhibited low fouling due to effective fabrication techniques, the optimization of operational parameters during processing could further increase transmembrane pressure by maximizing flux at the same time reducing fouling of membrane including increase in cross-flow velocity.

Funding

This research was jointly funded by the Ministry of Higher Education Malaysia awarded to Universiti Sains Malaysia; Fundamental Research Grant Scheme with Project Code: FRGS/1/2019/STG07/USM/02/12 and Universiti Tun Hussein Onn Malaysia. The authors would like to thank the Ministry of Higher Education Malaysia (KPM) for providing the Fundamental Research Grant Scheme (FRGS) with reference code FRGS/1/2019/WAB05/UTHM/02/5, Modification of Bead Adsorbents with Ceramic Sanitary Ware Waste (CSWW) and Chitosan for Laundry Greywater (LGW) Safe Disposal for the full financial support for this research project.

Acknowledgement

The authors would like to thank the collaboration between Universiti Sains Malaysia Penang, Malaysia and Universiti Tun Hussein Onn Malaysia, Johor Malaysia, which has made this work possible.

References

[1] A.A. Oyekanmi, A.A.A. Latiff, Z. Daud, R.M.S. Radin Mohamed, N.A.A. Aziz, N. Ismail, M. Rafatullah, A. Ahmad, K. Hossain, Adsorption of pollutants from palm oil mill effluent using natural adsorbents: optimization and isotherm studies, Desal. Water Treat., 169 (2019) 181–90.

[2] A.R.O. Adeleke, A.A.A. Latiff, Z. Daud, N.F.M. Daud, M.K. Aliyu, Heavy metal removal from wastewater of palm oil mill using developed activated carbon from coconut shell and cow bones, Key Eng. Mater., 737 (2017) 428–432.

[3] A.A. Oyekanmi, A.A.A. Latiff, Z. Daud, N.F.M. Daud, P. Gani, Adsorption of heavy metal from palm oil mill effluent on the mixed media used for the preparation of composite adsorbent, IOP Conf. Ser.: Mater. Sci. Eng., 103 (2017) 06020, doi: 10.1051/matecconf/201710306020.

[4] D. Rana, T. Matsuura, Membrane Transport Models, In: Encyclopedia of Agriculture, Food, and Biological Engineering, Vol. 2, CRC Press, Boca Raton, Florida USA, 2010, pp. 1041–1047.

[5] D. Rana, T. Matsuura, S. Sourirajan, Physicochemical and Engineering Properties of Food in Membrane Separation Processes, In: Engineering Properties of Foods, Taylor & Francis, Boca Raton, CRC Press, Florida, USA, 2014, pp. 1041–1047.

[6] D. Rana, T. Matsuura, State of the art reviews in membrane science and research, J. Membr. Sci., 3 (2017) 118–119.

[7] N.D. Trung, N. Tri, P.H. Phuong, H.C. Anh, Synthesis of highly active heterostructured Al_2TiO_5/TiO_2 photocatalyst in a neutral medium, J. Nanomater., 2020 (2020) 1–12, doi: 10.1155/2020/6684791.

[8] Y.-H. Park, T. Hinoki, A. Kohyama, Development of multifunctional NITE-porous SiC for ceramic insulators, J. Nucl. Mater., 386–388 (2009) 1014–1017.

[9] L. Xu, X. Xi, W. Zhu, A. Shui, W.B. Dai, Investigation on the influence factors for preparing mullite-whisker-structured porous ceramic, J. Alloys Compd., 649 (2015) 739–745.

[10] Y.-H. Park, J.-S. Park, T. Hinoki, A. Kohyama, Development of manufacturing method for NITE-porous SiC ceramics using decarburization process, J. Eur. Ceram. Soc., 28 (2008) 657–661.

[11] W. Qin, B. Lei, C. Peng, J. Wu, Corrosion resistance of ultra-high purity porous alumina ceramic support, Mater. Lett., 144 (2015) 74–77.

[12] B. Hofs, J. Ogier, D. Vries. E.F. Beerendonk, E.R. Cornelissen, Comparison of ceramic and polymeric membrane permeability and fouling using surface water, Sep. Purif. Technol., 79 (2011) 365–374.

[13] H.T. Vo, J. Kim, N.Y. Lim, J.K. Lee, J.B. Joo, Effect of pore texture property of mesoporous alumina on adsorption performance of ammonia gas, J. Ind. Eng. Chem., 91 (2020) 129–138.

[14] A.A. Oyekanmi, A.A.A. Latiff, Z. Daud, R.M.S. Radin Mohamed, I. Norli, A.A. Aziz, M. Rafatullah, A. Akil, K. Hossain, A.K. Abiodun, Adsorption of cadmium and lead from palm oil mill effluent using bone-composite: optimisation and isotherm studies, Int. J. Environ. Anal. Chem., 99 (2019) 707–725.

[15] A.O. Adeleke, A.A. Latiff, Z. Daud, N.F.M. Daud, B. Ridzuan, Remediation of raw wastewater of palm oil mill using activated cow bone powder through batch adsorption, Key Eng. Mater., 705 (2016) 380–384.

[16] J. Kim, H. Lee, H.T. Vo, G. Lee, G.N. Kim, S. Jang, J.B. Joo, Bead-shaped mesoporous alumina adsorbents for adsorption of ammonia, Materials, 13 (2020) 1–13, doi: 10.3390/ma13061375.

[17] H. Khan, K. Gul, B. Ara, A. Khan, N. Ali, N. Ali, M. Bilal, Adsorptive removal of acrylic acid from the aqueous environment using raw and chemically modified alumina: batch adsorption, kinetic, equilibrium and thermodynamic studies, J. Environ. Chem. Eng., 8 (2020) 1–11, doi: 10.1016/j.jece.2020.103927.

[18] S. Suganuma, K. Arita, F. Nakano, E. Tsuji, N. Katada, Adsorption kinetics in removal of basic nitrogen-containing compounds from practical heavy oils by amorphous silica-alumina, Fuel, 266 (2020) 1–8, doi: 10.1016/j.fuel.2020.117055.

[19] M.A. Rosli, Z. Daud, A.A.A. Latiff, S.E. Rahman, A.A. Oyekanmi, H. Awang, A. Zainorabidin, A.A. Halim, The effectiveness of peat-AC composite adsorbent in removing SS, colour and Fe from landfill leachate, Int. J. Integr. Eng., 9 (2017) 1–4.

[20] A. Shaga, P. Shen, L.-G. Xiao, R.-F. Guo, Y.-B. Liu, Q.-C. Jiang, High damage-tolerance bio-inspired ZL205A/SiC composites with a lamellar-interpenetrated structure, Mater. Sci. Eng., A, 708 (2017) 199–207.

[21] Y. Sun, Z. Yang, D. Cai, Q. Li, H. Li, S. Wang, D. Jia, Y. Zhuo, Mechanical, dielectric and thermal properties of porous boron nitride/silicon oxynitride ceramic composites prepared by pressureless sintering, Ceram. Int., 43(2017) 8230–8235.

[22] M.S. Rayat, S.S. Gill, R. Singh, L. Sharma, Fabrication and machining of ceramic composites — a review on current scenario, Mater. Manuf. Processes, 32 (2017) 1451–1474.

[23] A. Sommers, Q. Wang, X. Han, C. T'Joen, Y. Park, A. Jacobi, Ceramics and ceramic matrix composites for heat exchangers in advanced thermal systems—a review, Appl. Therm. Eng., 30 (2010) 1277–1291.

[24] R. Smyth, The Use of High Temperature Heat Exchangers to Increase Power Plant Thermal Efficiency, IECEC-97 Proceedings of the Thirty-Second Intersociety Energy Conversion Engineering Conference (Cat. No.97CH6203), IEEE, Honolulu, HI, USA, 1997.

[25] Z. He, Z. Lyu, Q. Gu, L. Zhang, J. Wang, Ceramic-based membranes for water and wastewater treatment, Colloids Surf., A, 578 (2019) 1–19, doi: 10.1016/j.colsurfa.2019.05.074.

[26] E.C. Hammel, O.L.-R. Ighodaro, O.I. Okoli, Processing and properties of advanced porous ceramics: an application based review, Ceram. Int., 40 (2014) 15351–15370.

[27] J.H. Huang, X.Q. Cheng, Q. Bai, Y.J. Zhang, K. Wang, J. Ma, L. Shao, Ultrafast poly(sodium methacrylate)-grafted UiO-66-incorporated nanocomposite membranes enable excellent active pharmaceutical ingredient concentration, Ind. Eng. Chem. Res., 60 (2021) 6287–6297.

[28] Y. Zhang, J. Guo, G. Han, Y. Bai, Q. Ge, J. Ma, L. Shao, Molecularly soldered covalent organic frameworks for ultrafast precision sieving, Sci. Adv., 7 (2021) 8706, doi: 10.1126/sciadv.abe8706.

[29] L. Shen, L. Tian, J. Zuo, X. Zhang, S. Sun, Y. Wang, Developing high-performance thin-film composite forward osmosis membranes by various tertiary amine catalysts for desalination, Adv. Compos. Mater., 2 (2019) 51–69.

[30] H. Hu, F. Ding, H. Ding, J. Liu, M. Xiao, Y. Meng, L. Sun, Sulfonated poly(fluorenyl ether ketone)/sulfonated α-zirconium phosphate nanocomposite membranes for proton exchange membrane fuel cells, Adv. Compos. Mater., 3 (2020) 498–507.

[31] T.T. Dele-Afolabi, M.A. Azmah Hanim, M. Norkhairunnisa, S. Sobri, R. Calin, Investigating the effect of porosity level and pore former type on the mechanical and corrosion resistance properties of agro-waste shaped porous alumina ceramics, Ceram. Int., 43 (2017) 8743–8754.

[32] H. Fang, J.F. Gao, H.T. Wang, C.S. Chen, Hydrophobic porous alumina hollow fiber for water desalination via membrane distillation process, J. Membr. Sci., 403 (2012) 41–46.

[33] T.T. Dele-Afolabi, M.A. Azmah Hanim, M. Norkhairunnisa, S. Sobri, R. Calin, Z.N. Ismarrubie, Significant effect of rice husk and sugarcane bagasse pore formers on the microstructure and mechanical properties of porous Al_2O_3/Ni composites, J. Alloys Compd., 743 (2018) 323–331.

[34] Y. Wang, X. Wang, C. Liu, X. Su, C. Yu, Y. Su, L. Qiao, Y. Bai, Aluminum titanate based composite porous ceramics with both high porosity and mechanical strength prepared by a special two-step sintering method, J. Alloys Compd., 853 (2021) 1–9, doi: 10.1016/j.jallcom.2020.157193.

[35] R.M. Khattab, M.A. Hessien, N.I. Abd El Ghaffar, S.H. Abd El Rahim, H.E.H. Sadek, Porous alumina-felsite ceramic composites prepared by direct coagulation casting method: felsite rock (central-eastern desert, Egypt), Ceram. Int., 46 (2020) 28308–28315.

[36] Y.H. Cho, S. Jeong, S.-J. Kim, Y. Kim, H.J. Lee, T.H. Lee, H.B. Park, H. Park, S.-E. Nam, Y.-I. Park, Sacrificial graphene oxide interlayer for highly permeable ceramic thin film composite membranes, J. Membr. Sci., 618 (2021) 1–10, doi: 10.1016/j.memsci.2020.118442.

[37] D. Li, Q. Yu, J. Li, L. Zeng, S. Gao, Manufacture of Si_3N_4-SiCN composite bulks with hierarchical pore structure, J. Eur. Ceram. Soc., 41 (2021) 284–289.

[38] C.M. Guzzo, J.A. Nychka, Bone 'spackling' paste: mechanical properties and *in vitro* response of a porous ceramic composite bone tissue scaffold, J. Mech. Behav. Biomed. Mater., 112 (2020) 103958, doi: 10.1016/j.jmbbm.2020.103958.

[39] Y. Wu, Z. Yang, N. Wu, S. Zhao, J. Li, Y. Li, Design of three-dimensional interconnected porous hydroxyapatite ceramic-based composite phase change materials for thermal energy storage, Int. J. Energy Res., 44 (2020) 11930–11940.

[40] H. Shao, X. Yu, Z. Zhang, T. Lin, J. Peng, A. Wang, S. Liu, M. Zhao, Effect of different $CaSO_4$ contents on $CaSiO_3$-$CaSO_4$ porous composite bone scaffolds by 3D gel-printing, Int. J. Appl. Ceram. Technol., 17 (2020) 2762–2767.

[41] M. Biernat, L. Ciołek, M. Dzierżyńska, A. Oziębło, J. Sawicka, M. Deptuła, M. Bauer, W. Kamysz, M. Pikuła, Z. Jaegermann, S. Rodziewicz-Motowidło, Porous chitosan/ZnO-doped bio-glass composites as carriers of bioactive peptides, Int. J. Appl. Ceram. Technol., 17 (2020) 2807–2816.

[42] H. Shao, X. Yu, Z. Zhang, T. Lin, J. Peng, A. Wang, S. Liu, M. Zhao, Effect of different $CaSO_4$ contents on $CaSiO_3$-$CaSO_4$

porous composite bone scaffolds by 3D gel-printing, Int. J. Appl. Ceram. Technol., 17 (2020) 2762–2767.

[43] ASTM. Standard, A, E112–13, Standard Test Methods for Determining Average Grain Size, 2013.

[44] M.L. Sandoval, M.H. Talou, A.G. Tomba Martinez, M.A. Camerucci, Mechanical testing of cordierite porous ceramics using high temperature diametral compression, J. Mater. Sci., 45 (2010) 5109–5117.

[45] ASTM. Standard, Standard Test Methods for Apparent Porosity, Water Absorption, Apparent Specific Gravity, and Bulk Density of Burned Refractory Brick and Shapes by Boiling Water, West Conshohocken, PA.: ASTM C20–00, 2015.

[46] S.G. Cook, J.A. Little, J.E. King, Etching and microstructure of engineering ceramics, Mater. Charact., 34 (1995) 1–8.

[47] T.T. Dele-Afolabi, M.A.A. Hanim, M. Norkhairunnisa, S. Sobri, R. Calin, O.J. Ojo-Kupoluyi, Fabrication Methods and Characterization Techniques for Porous Ceramic Materials, In: Reference Module in Materials Science and Materials Engineering, Elsevier Encyclopaedia, United Kingdom, 2019.

[48] R. Barkallah, R. Taktak, N. Guermazi, F. Zaïri, J. Bouaziz, F. Zaïri, Manufacturing and mechanical characterization of Al_2O_3/β-TCP/TiO_2 biocomposite as a potential bone substitute, Int. J. Adv. Manuf. Syst., 95 (2018) 3369–3380.

[49] J.B. Zhu, T. Zhou, Z.Y. Liao, L. Sun, X.B. Li, R. Chen, Replication of internal defects and investigation of mechanical and fracture behaviour of rock using 3D printing and 3D numerical methods in combination with X-ray computerized tomography, Int. J. Rock Mech. Min. Sci., 106 (2018) 198–212.

[50] I. Deniz Akin, W. Likos, Brazilian tensile strength testing of compacted clay, Geotech. Test. J., 40 (2017) 608–617.

[51] C. ASTM, Standard Test Method for Splitting Tensile Strength of Cylindrical Concrete Specimens, West Conshohocken, PA, 2011.

[52] R.C. Hibbeler, Statics and Mechanics of Materials, Pearson Higher Ed., Hibbeler Pearson Prentice Hall, Saddle River, NJ, 2013.

[53] J.L. Amorós, V. Cantavella, J.C. Jarque, C. Felíu, Green strength testing of pressed compacts: an analysis of the different methods, J. Eur. Ceram. Soc., 28 (2008) 701–710.

[54] T.V. Vineeth Kumar, M.D. Prashanth, Evaluation of the strength of cast iron using diametral compression test, Mater. Today:. Proc., 4 (2017) 9956–9960.

[55] M.L. Sandoval, M.H. Talou, A.G.T. Martinez, M.A. Camerucci, E. Gregorová, W. Pabst, Porous cordierite-based ceramics processed by starch consolidation casting – microstructure and high-temperature mechanical behavior, Ceram. Int., 44 (2018) 3893–3903.

[56] M.L. Sandoval, M.H. Talou, A.G.T. Martinez, M.A. Camerucci, E. Gregorová, W. Pabst, High-temperature mechanical behavior of cordierite-based porous ceramics prepared by modified cassava starch thermogelation, J. Mater. Sci., 47 (2012) 8013–8021.

[57] M. Fahad, Stresses and failure in the diametral compression test, J. Mater. Sci., 31 (1996) 3723–3729.

[58] M.L. Sandoval, M.A. Pucheu, M.H. Talou, A.G. Tomba Martinez, M.A. Camerucci, Mechanical evaluation of cordierite precursor green bodies obtained by starch thermogelling, J. Eur. Ceram. Soc., 29 (2009) 3307–3317.

[59] D. Buncianu, N. Tessier-Doyen, J. Absi, R. Negru, D.-A. Şerban, L. Marşavina, Multi-scale mechanical behaviour of a highly porous alumina based foam, Met. Mater. Int., 26 (2020) 1524–1532.

[60] G. Zhang, L. Ma, B. Wang, L. Wu, Mechanical behaviour of CFRP sandwich structures with tetrahedral lattice truss cores, Composites, Part B, 43 (2012) 471–476.

[61] J.R. Woodard, A.J. Hilldore, S.K. Lan, C.J. Park, A.W. Morgan, J.A.C. Eurell, S.G. Clark, M.B. Wheeler, R.D. Jamison, A.J. Wagoner Johnson, The mechanical properties and osteoconductivity of hydroxyapatite bone scaffolds with multi-scale porosity, Biomaterials., 28 (2007) 45–54.

[62] C.Q. Dam, R. Brezny, D.J. Green, Compressive behavior and deformation-mode map of an open cell alumina, J. Mater. Res., 5 (1990) 163–171.

[63] ASTM, I., Standard Test Method for Vickers Indentation Hardness of Advanced Ceramics, ASTM Standards, West Conshohocken, 2015.

[64] P. Ramavath, P. Biswas, N. Ravi, R. Johnson, E. Harkin-Jones, Prediction and validation of buckling stress (σ_{crt}) of the ceramic honeycomb cell walls under quasi-static compression, Cogent Eng., 3 (2016) 1–8, doi: 10.1080/23311916.2016.1168068.

[65] G.D. Quinn, Weibull strength scaling for standardized rectangular flexure specimens, J. Am. Ceram. Soc., 86 (2003) 508–510.

[66] G.D. Quinn, B.T. Sparenberg, P. Koshy, L.K. Ives, S. Jahanmir, D.D. Arola, Flexural strength of ceramic and glass rods, J. Test. Eval., 37 (2009) 222–244.

[67] T.T. Dele-Afolabi, M.A. Azmah Hanim, M. Norkhairunnisa, S. Sobri, R. Calin, Z.N. Ismarrubie, Tensile strength and corrosion resistance properties of porous Al_2O_3/Ni composites prepared with rice husk pore-forming agent, Ceram. Int., 44 (2018) 11127–11135.

[68] O. Abdulrahman Adeleke, A.A.A. Latiff, M.R. Saphira, Z. Daud, I. Norli, A. Ahsan, N. Adila Ab Aziz, A. Al-Gheethi, V. Kumar, A. Fadilat, N. Apandi, Principles and Mechanism of Adsorption for the Effective Treatment of Palm Oil Mill Effluent for Water Reuse, A. Ahsan, A. Fauzi Ismail, Eds., Nanotechnology in Water and Wastewater Treatment, Elsevier, London, 2019, pp. 1–33.

[69] M.A. Rosli, Z. Daud, M.B. Ridzuan, N.A. Abd Aziz, H.B. Awang, A.O. Adeleke, K. Hossain, N. Ismail, Equilibrium isotherm and kinetic study of the adsorption of organic pollutants of leachate by using micro peat-activated carbon composite media, Desal. Water Treat., 160 (2019) 185–192.

[70] Y. Zhao, G. Huang, C. An, J. Huang, X. Xin, X. Chen, Y. Hong, P. Song, Removal of *Escherichia coli* from water using functionalized porous ceramic disk filter coated with Fe/TiO_2 nano-composites, J. Water Process Eng., 33 (2020) 101013, doi: 10.1016/j.jwpe.2019.101013.

[71] T.-F. Lin, J.-K. Wu, Adsorption of arsenite and arsenate within activated alumina grains: equilibrium and kinetics, Water Res., 35 (2001) 2049–2057.

[72] S. Mor, K. Ravindra, N.R. Bishnoi, Adsorption of chromium from aqueous solution by activated alumina and activated charcoal, Bioresour. Technol., 98 (2007) 954–957.

[73] T.K. Naiya, A.K. Bhattacharya, S.K. Das, Adsorption of Cd(II) and Pb(II) from aqueous solutions on activated alumina, J. Colloid Interface Sci., 333 (2009) 14–26.

[74] Y. Ji, L. Li, Y.-T. Wang, Selenium removal by activated alumina in batch and continuous-flow reactors, Water Environ. Res., 92 (2020) 51–59.

[75] O. AbdulrahmanvAdeleke, A.A.A. Latiff, M.R. Saphira, Z. Daud, I. Norli, A. Ahsan, N Adila Ab Aziz, M. Ndah, V. Kumar, A. Al-Gheethi, M Arif Rosli, H. Mahmood, 2 – Locally Derived Activated Carbon From Domestic, Agricultural and Industrial Wastes for the Treatment of Palm Oil Mill Effluent, A. Ahsan, A.F. Ismail, Eds., Nanotechnology in Water and Wastewater Treatment: Theory and Applications Micro and Nano Technologies, Elsevier, London, 2019, pp. 35–62.

[76] R. Mohamed, A. Al-Gheethi, A. Abdulrahman, M.S. Bin Sainudin, S.A. Bakar, A.H.M. Kassim, Optimization of ceramic waste filter for bathroom greywater treatment using central composite design (CCD), J. Environ. Chem. Eng., 6 (2018) 1578–1588.

[77] J.-H. Ha, S.Z.A. Bukhari, J. Lee, I.-H. Song, C. Park, Preparation processes and characterizations of alumina-coated alumina support layers and alumina-coated natural material-based support layers for microfiltration, Ceram. Int., 42 (2016) 13796–13804.

[78] K. Gao, R. Cui, Y. Fan, X. Zhou, Y. Zhang, Low-cost pyrophyllite-based microfluidic device for the study of enhanced oil recovery, Micro Nano Lett., 14 (2019) 1349–1354.

[79] R. Ahmad, M. Aslam, E. Park, S. Chang, D. Kwon, J. Kim, Submerged low-cost pyrophyllite ceramic membrane filtration combined with GAC as fluidized particles for industrial wastewater treatment, Chemosphere, 206 (2018) 784–792.

[80] S. Chang, D. Kwon, J. Kim, New Approach with Fluidized Bed Reactor Using Low-Cost Pyrophyllite/Alumina Composite Membrane for Real-Metal Plating Wastewater Treatment, V. Naddeo, M. M. Balakrishnan, K.H. Choo, Eds., Frontiers in Water-Energy-Nexus—Nature-Based Solutions, Advanced Technologies and Best Practices for Environmental Sustainability, Springer, Cham, 2020, pp. 177–178.

[81] P. Chen, X. Ma, Z. Zhong, F. Zhang, W. Xing, Y. Fan, Performance of ceramic nanofiltration membrane for desalination of dye solutions containing NaCl and Na_2SO_4, Desalination, 404 (2017) 102–111.

[82] J. Kim, B. Van der Bruggen, The use of nanoparticles in polymeric and ceramic membrane structures: review of manufacturing procedures and performance improvement for water treatment, Environ. Pollut., 158 (2010) 2335–2349.

[83] R. Vinoth Kumar, A.K. Ghoshal, G. Pugazhenthi, Elaboration of novel tubular ceramic membrane from inexpensive raw materials by extrusion method and its performance in microfiltration of synthetic oily wastewater treatment, J. Membr. Sci., 490 (2015) 92–102.

[84] X. Chen, T. Qi, Y. Zhang, T. Wang, M. Qiu, Z. Cui, Y. Fan, Facile pore size tuning and characterization of nanoporous ceramic membranes for the purification of polysaccharide, J. Membr. Sci., 597 (2020) 117631, doi: 10.1016/j.memsci.2019.117631.

[85] L. Zhu, X. Dong, M. Xu, F. Yang, M.D. Guiver, Y. Dong, Fabrication of mullite ceramic-supported carbon nanotube composite membranes with enhanced performance in direct separation of high-temperature emulsified oil droplets, J. Membr. Sci., 582 (2019) 140–150.

[86] R. Mouratib, B. Achiou, M. El Krati, S.A. Younssi, S. Tahiri, Low-cost ceramic membrane made from alumina- and silica-rich water treatment sludge and its application to wastewater filtration, J. Eur. Ceram. Soc., 40 (2020) 5942–5950.

[87] K. Xia, S. Yu, Y. Li, H. Han, L. Duan, Z. Hou, X. Liu, The surface carboxyl group of carbonaceous microspheres effects on the synthesis and structure of SiOC ceramics, J. Eur. Ceram. Soc., 41 (2021) 2375–2385.

[88] O.A. Fomina, A. Yu. Stolboushkin, Modeling of the transition layer in ceramic matrix composites from coal wastes and clay, Solid State Phenom., 299 (2020) 37–42.

[89] D. Li, B. Tang, X. Lu, W. Chen, X. Dong, J. Wang, X. Wang, Hierarchically carbonized silk/ceramic composites for electro-thermal conversion, Composites, Part A, 141 (2021) 106237, doi: 10.1016/j.compositesa.2020.106237.

[90] W. Liu, D. Wang, R.A. Soomro, F. Fu, N. Qiao, Y. Yu, R. Wang, B. Xu, Ceramic supported attapulgite-graphene oxide composite membrane for efficient removal of heavy metal contamination, J. Membr. Sci., 591 (2019) 117323, doi: 10.1016/j.memsci.2019.117323.

[91] L. Liang, J. Fan, M. Wang, G. Chen, G. Sun, Ternary thermoelectric composites of polypyrrole/PEDOT:PSS/carbon nanotube with unique layered structure prepared by one-dimensional polymer nanostructure as template, Compos. Sci. Technol., 187 (2020) 107948, doi: 10.1016/j.compscitech.2019.107948.

[92] C. Liu, J. Xia, J. Gu, W. Wang, Q. Liu, L. Yan, T. Chen, Multifunctional CNTs-PAA/MIL101(Fe)@Pt composite membrane for high-throughput oily wastewater remediation, J. Hazard. Mater., 403 (2021) 123547, doi: 10.1016/j.jhazmat.2020.123547.

[93] B. Arora, P. Attri, Carbon nanotubes (CNTs): a potential nanomaterial for water purification, J. Compos. Sci., 4 (2020) 135, doi: 10.3390/jcs4030135.

[94] L. Yan, C. Liu, J. Xia, M. Chao, W. Wang, J. Gu, T. Chen, CNTs/TiO_2 composite membrane with adaptable wettability for on-demand oil/water separation, J. Cleaner Prod., 275 (2020) 124011, doi: 10.1016/j.jclepro.2020.124011.

[95] E. Elnabawy, I.M.A. Elsherbiny, A.M.A. Abdelsamad, B. Anis, A. Hassan, M. Ulbricht, A.S.G. Khalil, Tailored CNTs buckypaper membranes for the removal of humic acid and separation of oil-in-water emulsions, Membranes, 10 (2020) 97, doi: 10.3390/membranes10050097.

[96] N. Chaukura, R. Chiworeso, W. Gwenzi, M.M. Motsa, W. Munzeiwa, W. Moyo, I. Chikurunhe, T.T.I. Nkambule, A new generation low-cost biochar-clay composite 'biscuit' ceramic filter for point-of-use water treatment, Appl. Clay Sci., 185 (2020) 105409, doi: 10.1016/j.clay.2019.105409.

[97] T. Wu, B. Zhou, T. Zhu, J. Shi, Z. Xu, C. Hu, J. Wang, Facile and low-cost approach towards a PVDF ultrafiltration membrane with enhanced hydrophilicity and antifouling performance *via* graphene oxide/water-bath coagulation, RSC Adv., 5 (2015) 7880–7889.

[98] M. Kárászová, M. Bourassi, J. Gaálová, Membrane removal of emerging contaminants from water: which kind of membranes should we use?, Membranes, 10 (2020) 305, doi: 10.3390/membranes10110305.

[99] A. Faivre, F. Despetis, L. Duffours, P. Colombel, Effect of CaO and Al_2O_3 addition on the properties of $K_2O–Na_2O–P_2O_5$ glass system, Int. J. Appl. Glass Sci., 10 (2019) 162–171.

[100] K.S.D. Premarathna, A.U. Rajapaksha, N. Adassoriya, B. Sarkar, N.M.S. Sirimuthu, A. Cooray, Y.S. Ok, M. Vithanage, Clay-biochar composites for sorptive removal of tetracycline antibiotic in aqueous media, J Environ Manage., 218 (2019) 315–322.

[101] G.-T. Lim, H.-G. Jeong, I.-S. Hwang, D.-H. Kim, N. Park, J. Cho, Fabrication of a silica ceramic membrane using the aerosol flame deposition method for pretreatment focusing on particle control during desalination, Desalination, 238 (2009) 53–59.

[102] J. Yang, X. Xing, Y. Zhao, R. Mu, Y. Guo, H. Hou, Microstructures of nickel-doped methylated silica membrane materials calcined in air: influence of Ni content, Ferroelectrics, 562 (2020) 85–95.

[103] M. Panchal, G. Raghavendra, M. Omprakash, S. Ojha, Fabrication and characterization of silica based ceramic composite for filtration applications, Silicon, 13 (2021) 1951–1960.

[104] F. Ali, S.B. Khan, N. Shaheen, Y.Z. Zhu, Eggshell membranes coated chitosan decorated with metal nanoparticles for the catalytic reduction of organic contaminates, Carbohydr. Polym., 259 (2021) 117681, doi: 10.1016/j.carbpol.2021.117681.

[105] W. Puthai, M. Kanezashi, H. Nagasawa, T. Tsuru, T. Puthai, Nanofiltration performance of SiO_2-ZrO_2 membranes in aqueous solutions at high temperatures, Sep. Purif. Technol., 168 (2016) 238–247.

[106] J. Zhang, T. Liu, Q. Huang, Z. Luo, A. Lu, L. Zhu, Preparation, properties characterization and structure formation mechanism of silica sand tailings-based ceramic materials, Mater. Chem. Phys., 255 (2020) 123611, doi: 10.1016/j.matchemphys.2020.123611.

[107] Z. Wang, X. Lyu, G. Yao, P. Wu, J. Wang, J. Wei, Preparation of Ca–Si–Al–Mg porous ceramics by Co-operation of Ca&Mg-contained soda residue and altered rock gold tailings, J. Cleaner Prod., 262 (2020) 121345, doi: 10.1016/j.jclepro.2020.121345.

[108] S.S. Alias, Z. Harun, N. Manoh, M.R. Jamalludin, Effects of temperature on rice husk silica ash additive for fouling mitigation by polysulfone–RHS ash mixed-matrix composite membranes, Polym. Bull., 77 (2020) 4043–4075.

[109] E.P. Ferreira-Neto, S. Ullah, M.B. Simões, A.P. Perissinotto, F.S. de Vicente, P.-L.M. Noeske, S.J.L. Ribeiro, U.P. Rodrigues-Filho, Solvent-controlled deposition of titania on silica spheres for the preparation of SiO_2@TiO_2 core@shell nanoparticles with enhanced photocatalytic activity, Colloids Surf., A, 570 (2019) 293–305.

[110] A. Oun, N. Tahri, S. Mahouche-Chergui, B. Carbonnier, S. Majumdar, S. Sarkar, G.C. Sahoo, R. Ben Amar, Tubular ultrafiltration ceramic membrane based on titania nanoparticles immobilized on macroporous clay-alumina support: elaboration, characterization and application to dye removal, Sep. Purif. Technol., 188 (2017) 126–133.

[111] M. Shokouhfar, S.R. Allahkaram, Formation mechanism and surface characterization of ceramic composite coatings on pure titanium prepared by micro-arc oxidation in electrolytes

containing nanoparticles, Surf. Coat. Technol., 291 (2016) 396–405.
[112] X. Zhang, L. Xu, S. Du, W. Han, J. Han, Preoxidation and crack-healing behavior of ZrB_2–SiC ceramic composite, J. Am. Ceram. Soc., 91 (2008) 4068–4073.
[113] F. Mohsenifar, H. Ebrahimifar, Effect of titanium oxide ceramic particles concentration on microstructure and corrosion behaviour of Ni–P–Al_2O_3–TiO_2 composite coating, Bull. Mater. Sci., 43 (2020) 99, doi: 10.1007/s12034-020-2068-x.
[114] H. Sun, Y. Wu, Y. Jin, Y. Lv, G. Ju, L. Chen, Y. Hu, Photocatalytic titanium dioxide immobilized on an ultraviolet emitting ceramic substrate for water purification, Mater. Lett., 240 (2019) 100–102.
[115] V.G. Deshmane, Y.G. Adewuyi, Synthesis of thermally stable, high surface area, nanocrystalline mesoporous tetragonal zirconium dioxide (ZrO_2): effects of different process parameters, Microporous Mesoporous Mater., 148 (2012) 88–100.
[116] K. Li, K.J. Chen, J. Peng, S. Koppala, M. Omran, G. Chen, One-step preparation of CaO-doped partially stabilized zirconia from fused zirconia, Ceram. Int., 46 (2020) 6484–6490.
[117] A. Fakeeha, A.A. Ibrahim, H. Aljuraywi, Y. Alqahtani, A. Alkhodair, S. Alswaidan, A.E. Abasaeed, S.O. Kasim, S. Mahmud, A.S. Al-Fatesh, Hydrogen production by partial oxidation reforming of methane over Ni catalysts supported on high and low surface area alumina and zirconia, Processes, 8 (2020) 499, doi: 10.3390/pr8050499.
[118] M. Boussemghoune, M. Chikhi, F. Balaska, Y. Ozay, N. Dizge, B. Kebabi, Preparation of a zirconia-based ceramic membrane and its application for drinking water treatment, Symmetry, 12 (2020) 933, doi: 10.3390/sym12060933.
[119] C. Belviso, State-of-the-art applications of fly ash from coal and biomass: a focus on zeolite synthesis processes and issues, Prog. Energy Combust. Sci., 65 (2018) 109–135.
[120] A.K. Basumatary, R.V. Kumar, A.K. Ghoshal, G. Pugazhenthi, Cross flow ultrafiltration of Cr(VI) using MCM-41, MCM-48 and faujasite (FAU) zeolite-ceramic composite membranes, Chemosphere, 153 (2016) 436–446.
[121] J. Zheng, Q. Zeng, Y. Zhang, Y. Wang, J. Ma, X. Zhang, W. Sun, R. Li, Hierarchical porous zeolite composite with a core−shell structure fabricated using β-zeolite crystals as nutrients as well as cores, Chem. Mater., 22 (2010) 6065–6074.
[122] J. Yu, C. Qi, J. Zhang, C. Bao, H. Xu, Synthesis of a zeolite membrane as a protective layer on a metallic Pd composite membrane for hydrogen purification, J. Mater. Chem., 9 (2015) 5000–5006.
[123] H. Ma, Z. Zhu, P. Tang, T. Su, P. Wu, H. Lü, Hierarchical Ti-Beta zeolites with uniform intracrystalline mesopores hydrothermally synthesized via interzeolite transformation for oxidative desulfurization, Microporous Mesoporous Mater., 311 (2021) 110702, doi: 10.1016/j.micromeso.2020.110702.
[124] Q. Jiang, J. Zhou, Y. Miao, S. Yang, M. Zhou, Z. Zhong, W. Xing, Lower-temperature preparation of SiC ceramic membrane using zeolite residue as sintering aid for oil-in-water separation, J. Membr. Sci., 610 (2020) 118238, doi: 10.1016/j.memsci.2020.118238.
[125] O.T. Opafola, A.O. David, F.O. Ajibade, H.O. Adeyemi, O.I. Solana, B.D. Odugbose, The utilization of bentonite enhanced termite mound soil mixture as filter for the treatment of paint industrial effluent, SN Appl. Sci., 3 (2021) 415, doi: 10.1007/s42452-021-04405-x.
[126] P.-K. Shih, W.-L. Chang, The effect of water purification by oyster shell contact bed, Ecol. Eng., 77 (2015) 382–390.
[127] S. Tong, J.L. Stocks, L.C. Rodriguez-Gonzalez, C. Feng, S.J. Ergas, Effect of oyster shell medium and organic substrate on the performance of a particulate pyrite autotrophic denitrification (PPAD) process, Bioresour. Technol., 244 (2017) 296–303.
[128] H.Y. Yen, J.H. Chou, Water purification by oyster shell bio-medium in a recirculating aquaponic system. Ecol. Eng., 95 (2016) 229–236.
[129] J.N.G. Deutou, Van Essa L.S. Kamga, R.C. Kaze, E. Kamseu, V.M. Sglavo, Thermal behaviour and phases evolution during the sintering of porous inorganic membranes, J. Eur. Ceram. Soc., 40 (2020) 2151–2162.
[130] J.-H. Ha, S.Z.A. Bukhari, J. Lee, I.-H. Song, C. Park, Preparation processes and characterizations of alumina-coated alumina support layers and alumina-coated natural material-based support layers for microfiltration, Ceram. Int., 42 (2016) 13796–13804.
[131] F. Lin, S. Zhang, G. Ma, L. Qiu, H. Sun, Application of ceramic membrane in water and wastewater treatment, E3S Web Conf., 53 (2018) 04032, doi: 10.1051/e3sconf/20185304032.
[132] S. Roy, S. Majumdar, G.C. Sahoo, S. Bhowmick, A.K. Kundu, P. Mondal, Removal of As(V), Cr(VI) and Cu(II) using novel amine functionalized composite nanofiltration membranes fabricated on ceramic tubular substrate, J. Hazard. Mater., 399 (2020) 122841, doi: 10.1016/j.jhazmat.2020.122841.